

Finite-temperature reaction-rate formula: Finite-volume system, detailed balance, $T \rightarrow 0$ limit, and cutting rules

A. Niégawa*

Department of Physics, Osaka City University, Sumiyoshi-ku, Osaka 558, Japan

(Received 23 June 1997; revised manuscript received 9 September 1997; published 24 December 1997)

A complete derivation, from first principles, of the reaction-rate formula for a generic process taking place in a heat bath of finite volume is given. It is shown that the formula involves no finite-volume correction. Through perturbative diagrammatic analysis of the resultant formula, the detailed-balance formula is derived. The zero-temperature limit of the formula is discussed. Thermal cutting rules, which are introduced in previous work, are compared with those introduced by other authors. [S0556-2821(98)00903-5]

PACS number(s): 11.10.Wx, 12.38.Bx, 12.38.Mh

I. INTRODUCTION

Ultrarelativistic heavy-ion-collision experiments at CERN and the BNL Relativistic Heavy Ion Collider (RHIC) lead us to entertain a hope of reviving quark-gluon plasma (QGP) in the present day. As promising observables of the QGP formation, rates of various reactions taking place in a QGP (heat bath) have been computed by many authors. Almost all of them, however, concentrated on the analyses of particle production from a QGP or the decay rate of a particle in a QGP, whose computational method has long been known [1].

Since then, through analyses from first principles, a calculational scheme of the rate of a generic thermal reaction has been proposed [2–7]. The resultant reaction-rate formula is written in terms of the Keldish variant of the real-time formalism (RTF) of thermal field theory [8]. However, a complete analysis of classes of diagrams, which leads to diagrams in the RTF including thermal propagators with $n (\geq 2)$ thermal self-energy insertion, is still lacking. Reference [3] is the only work that discusses such classes of diagrams in scalar field theory. In the course of the deduction [3] of such diagrams, there comes about an involved series, for which an identity is assumed. As for [4], where fermion fields are dealt with, the set of diagrams under consideration is not analyzed. This is also the case¹ for [7]. Incidentally, the thermal self-energy part in itself and the one thermal self-energy-inserted propagator are deduced in [2–4,9].

The principal purpose of this paper is to present a complete derivation of the thermal reaction-rate formula (Secs. II–V).

There has been confusion regarding the issue of finite-volume corrections to the standard thermal perturbation theory. (Why and how has the confusion arisen is described historically in [10] with relevant references.) By employing a cubic system with periodic boundary conditions, it has been shown in [10] that *thermal expectation values* of normal-

ordered products of field operators can be chosen to be zero and there is no finite-volume correction in thermal amplitudes. It should be stressed that this statement is the statement within the RTF. The statement does not tell us whether or not the thermal reaction-rate formula deduced from first principles is free from finite-volume corrections. We shall derive in Secs. II–V the thermal reaction-rate formula for the finite-volume system and explicitly see that there is no finite-volume correction.

It should be emphasized that the absence of finite-volume corrections here as well as in [10] is rather academic since a cubic system with periodic boundary conditions is taken. For physical finite-volume system, there are [6] two sources entering the finite-volume effects in the thermal perturbation theory constructed on the basis of a (grand) canonical ensemble. One comes from the physically sensible boundary condition on the single-particle wave function. The other comes from taking the physically sensible ensemble. For the nonequilibrium case, such as an expanding QGP, the situation is of course much more involved.

In Sec. VI, through diagrammatic analysis for the reaction-rate formula, we derive the detailed-balance formula. In Sec. VII, we analyze the zero-temperature limit of the reaction-rate formula and reproduce a variant of the Cutkosky rules [11].

At zero temperature, the cutting (Cutkosky) rules [11] are a powerful device to investigate the imaginary or absorptive part of a scattering amplitude and a reaction rate like a scattering cross section. Then, it is natural to infer that a finite-temperature extensions of the cutting rules (thermal cutting rules) also plays an important role in thermal field theory.

Previously, several authors [12,2–7,9,13–16] have discussed thermal cutting rules.² However, because of the fact that the generalization of the notion of “cutting” in vacuum theory to the case of thermal field theory is not unique, the terms “cutting” and “(un)cuttable” are endowed with different meanings in [12,2–7,9,13–16], which has caused a

*Electronic address: niegawa@sci.osaka-cu.ac.jp

¹In fact, in [7], an $n (\geq 2)$ thermal self-energy-inserted propagator is not deduced from the starting formula but is assumed at the start to have the correct form in the RTF [cf. Eq. (17) in [7]].

²The relationship between a thermal self-energy part (in imaginary-time formalism) and a rate of decay (production) of a particle in (from) a heat bath was clarified in [1], from which the cutting rules as applied to the self-energy part can be read off.

recent controversy. With these circumstances in mind, we pigeonhole different definitions of thermal cutting rules (Sec. VIII).

II. PRELIMINARY

We consider a heat-bath system of temperature T , composed of the fields $\phi^{(\alpha)}$, with α labeling collectively a field type and its internal degree of freedom. We assume $T \gg m$ and ignore m (hot plasma). The system is inside a cube with volume $V=L^3$. Employing the periodic boundary conditions, we label the single-particle basis by its momentum $\mathbf{p}_k = 2\pi\mathbf{k}/L$, $k_j = 0, \pm 1, \pm 2, \dots, \pm \infty$ ($j=x, y, z$).

Physically interesting thermal reactions are of the following generic type:

$$\{A\} + \text{heat bath} \rightarrow \{B\} + \text{anything}. \quad (2.1)$$

Here $\{A\}$ and $\{B\}$ designate a group of particles, which are not thermalized, such as virtual photons and leptons. (Generalization to more general processes, where among $\{A\}$ and/or $\{B\}$ are $\phi^{(\alpha)}$'s, is straightforward and will be dealt with in Sec. V.) The reaction rate \mathcal{R} of the thermal process (2.1) is expressed [2–4] as a statistical average of the transition probability $W=S^*S$ (with S the S -matrix element) of the *zero-temperature* ($T=0$) process,

$$\{A\} + \{n_{\mathbf{k}}^{(\alpha)}\} \rightarrow \{B\} + \{n_{\mathbf{k}}^{(\alpha)'}\}, \quad (2.2)$$

where $\{n_{\mathbf{k}}^{(\alpha)}\}$ denotes the group of $\phi^{(\alpha)}$'s, which consists of the number $n_{\mathbf{k}}^{(\alpha)}$ of $\phi_{\mathbf{k}}^{(\alpha)}$ ($\phi^{(\alpha)}$ in a mode \mathbf{k}):

$$\mathcal{R} = \mathcal{N}/\mathcal{D}, \quad (2.3a)$$

$$\mathcal{N} \equiv \overline{\sum_{\{n_{\mathbf{k}}^{(\alpha)}\}} \rho \sum_{\{n_{\mathbf{k}}^{(\alpha)'}\}} \frac{W[\text{process (2.2)}]}{2\pi\delta(0)}}, \quad (2.3b)$$

$$\mathcal{D} \equiv \overline{\sum_{\{n_{\mathbf{k}}^{(\alpha)}\}} \rho \sum_{\{n_{\mathbf{k}}^{(\alpha)'}\}} W_0(\{n_{\mathbf{k}}^{(\alpha)}\} \rightarrow \{n_{\mathbf{k}}^{(\alpha)'}\})}, \quad (2.3c)$$

$$\rho = N^{-1} \exp\left(-\beta \sum_{\alpha} \sum_{\mathbf{k}} n_{\mathbf{k}}^{(\alpha)} p_{\mathbf{k}}\right). \quad (2.3d)$$

Here $\beta=1/T$, $p_{\mathbf{k}}=|\mathbf{p}_{\mathbf{k}}|$, and $2\pi\delta(0)=t_f-t_i(\sim\infty)$ is the time interval during which the interaction acts. $W_0=S_0^*S_0$, the ‘‘thermal vacuum bubble,’’ is the $T=0$ transition probability of the process indicated in Eq. (2.3c), i.e., the reaction among the heat-bath particles $\phi^{(\alpha)}$'s alone. Note that the perturbation series for \mathcal{D} starts from 1:

$$\mathcal{D} = 1 + \dots \quad (2.4)$$

In Eq. (2.3d), N is the normalization factor. In Eqs. (2.3b) and (2.3c), $\overline{\sum}$ stands for the summation with symmetry factors being respected, and, for a bosonic (fermionic) $\phi^{(\alpha)}$, $n_{\mathbf{k}}^{(\alpha)}$ runs over $0, 1, 2, \dots, \infty$ (0 and 1). It is to be noted that $\{A\}$ and $\{B\}$ in S , which we write $\{A, B\}_S$, are not necessarily involved in one connected part of S . This is also the case for $\{A, B\}_{S^*}$. We assume that, in $W=S^*S$, $\{A, B\}_S$ and $\{A, B\}_{S^*}$ are involved in one connected part, which we sim-

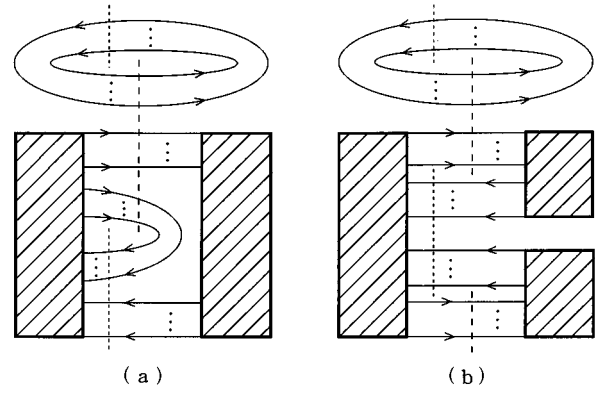


FIG. 1. Two examples of double-cut diagrams for the transition probability $W=S^*S$ in vacuum theory. Long dashed lines are the final-state cut lines while the short-dashed lines are the initial-state cut lines. The left side of the cut lines represents the S -matrix element S , while the right side does S^* . The line that is cut by the final-state (initial-state) cut line represents a particle in the final (initial) state in S . The lines cut by the initial-state [final-state] cut line include those corresponding to $\{A\}$ [$\{B\}$] in Eq. (2.2). The group of lines on top of the diagrams stands for spectator particles. (a) Both S and S^* are connected. In addition to the spectator particles mentioned above, additional spectator particles are in S^* . (b) S is connected while S^* is disconnected. Note, however, that S^*S is connected.

ply refer to as a connected W . Then, a connected W consists, in general, of two mutually disconnected parts; the one includes $\{A, B\}_S$ and $\{A, B\}_{S^*}$ and the other is a group of spectator particles. Generalization to other cases is straightforward. Examples of double-cut diagrams [17] for S^*S are depicted in Fig. 1. It should be remarked on the form of ρ in Eq. (2.3d). Let us recall the following two facts. On the one hand, the statistical ensemble is defined by the density matrix at the very initial time t_i ($\sim-\infty$). On the other hand, in constructing a perturbative RTF, an adiabatic switching off of the interaction is required [18,9,8]. Then, the Hamiltonian H in $\rho \equiv N^{-1}e^{-\beta H}$ should be the free Hamiltonian H_0 , which leads to Eq. (2.3d).

As will be seen below, diagrammatic analysis shows that \mathcal{N} , Eq. (2.3b), takes the form

$$\mathcal{N} = \mathcal{N}_{con} \mathcal{D}, \quad (2.5)$$

where \mathcal{N}_{con} corresponds to a connected diagram and \mathcal{D} is as in Eq. (2.3a). Then $\mathcal{R} = \mathcal{N}_{con}$.

The $T=0$ S -matrix element is obtained through an application of the reduction formula. As an illustration, we take a heat-bath system of thermal neutral scalars ϕ 's, and we take $\{A\}$ to be $\{\Phi(\mathbf{p}_i); i=1, \dots, m\}$ and $\{B\}$ to be $\{\Phi(\mathbf{q}_j); j=1, \dots, n\}$ with Φ a nonthermalized heavy neutral scalar. Assuming a Φ - ϕ coupling to be of the form $\Phi\phi'$, we have [2,3]

$$S = \prod_{j=1}^m (iK_{P_j, \Phi_j}) \prod_{k=1}^n (iK_{Q_k, \Phi_k}^*) \\ \times \prod_{\mathbf{k}} \left\{ \sum_{i_{\mathbf{k}}=0}^{n_{\mathbf{k}}} \sum_{i'_{\mathbf{k}}=0}^{n'_{\mathbf{k}}} \delta(n_{\mathbf{k}} - i_{\mathbf{k}}; n'_{\mathbf{k}} - i'_{\mathbf{k}}) \right\}$$

$$\begin{aligned} & \times N_{i_k i'_k}^{n_k n'_k} \prod_{n'=1}^{i'_k} (iK_{\mathbf{k},n'}^*) \prod_{n=1}^{i_k} (iK_{\mathbf{k},n}) \\ & \times \langle 0 | T \left[\prod_{n'=1}^{i'_k} \phi_{n'} \prod_{n=1}^{i_k} \phi_n \prod_{j=1}^m \Phi_j \prod_{k=1}^n \Phi_k \right] | 0 \rangle, \end{aligned} \quad (2.6)$$

where

$$N_{i_k i'_k}^{n_k n'_k} \equiv \left\{ \binom{n'_k}{i'_k} \binom{n_k}{i_k} \frac{1}{i'_k! i_k!} \right\}^{1/2}. \quad (2.7)$$

In Eq. (2.6), $\delta(\dots; \dots)$ denotes the Kronecker's δ symbol,

$$\begin{aligned} K_{\mathbf{k},n} \cdots \phi_n & \equiv \frac{1}{\sqrt{2p_{\mathbf{k}} V Z_{\Phi}}} \int d^4x e^{-ip_{\mathbf{k}} \cdot x} \square \cdots \phi(x), \\ K_{P_j, \Phi_j} \cdots \Phi_j & \equiv \frac{1}{\sqrt{2E_j V Z_{\Phi}}} \int d^4x e^{-iP_j \cdot x} \\ & \times (\square + M^2) \cdots \Phi_j(x), \end{aligned} \quad (2.8)$$

where $E_j = \sqrt{p_j^2 + M^2}$ with M the mass of Φ . The Z 's in Eq. (2.8) are the wave-function renormalization constants. S_0 in $W_0 = S_0^* S_0$ is given by a similar expression to Eq. (2.6), where factors related to the Φ fields are deleted. It is to be noted that, in Eq. (2.6), among $n_{\mathbf{k}}$ ($n'_{\mathbf{k}}$) of $\phi_{\mathbf{k}}$'s in the initial (final) state, $i_{\mathbf{k}}$ ($i'_{\mathbf{k}}$) of $\phi_{\mathbf{k}}$'s are absorbed in (emitted from) the $i_{\mathbf{k}}$ ($i'_{\mathbf{k}}$) vertices in S . The remaining $n_{\mathbf{k}} - i_{\mathbf{k}}$ ($= n'_{\mathbf{k}} - i'_{\mathbf{k}}$) of $\phi_{\mathbf{k}}$'s are merely spectators, which reflects only on the statistical factor in A in Eq. (3.14) below.

The expression for S^* , the complex conjugate of S , is obtained by taking the complex conjugate of Eq. (2.6), where we make the substitution

$$i_{\mathbf{k}} \rightarrow j_{\mathbf{k}} \quad i'_{\mathbf{k}} \rightarrow j'_{\mathbf{k}}.$$

This applies also to the expression for S_0^* .

III. DERIVATION OF THE REACTION-RATE FORMULA

In this section, we take self-interacting neutral scalar theory. Generalization to the complex-scalar theory is straightforward (cf. Sec. VIII). A comment on gauge theories is made at the end of this section. Fermion fields are dealt with in Sec. IV.

A. Analysis of non-mode-overlapping diagrams,

$$i_{\mathbf{k}} + i'_{\mathbf{k}} + j_{\mathbf{k}} + j'_{\mathbf{k}} \leq 2$$

In this subsection, for completeness, we briefly recapitulate the heart of the analysis of [2,3]. Let us analyze \mathcal{N} in Eq. (2.3b) with S in Eq. (2.6).

(a) $\{i_{\mathbf{k}} = i'_{\mathbf{k}} = j_{\mathbf{k}} = j'_{\mathbf{k}} = 0\}$. Let us take a diagram for $W = S^* S$. Let v_1 and v_2 be the vertices inside S , which are connected by the propagator

$$\frac{1}{V} \int_{-\infty}^{\infty} \frac{dp_0}{2\pi} \frac{i}{p^2 + i0^+}. \quad (3.1)$$

(b) $\{i_{\mathbf{k}} = i'_{\mathbf{k}} = 1, j_{\mathbf{k}} = j'_{\mathbf{k}} = 0\}$ and $\{i_{-\mathbf{k}} = i'_{-\mathbf{k}} = 1, j_{-\mathbf{k}} = j'_{-\mathbf{k}} = 0\}$. We first deal with the case $\{i_{\mathbf{k}} = i'_{\mathbf{k}} = 1, j_{\mathbf{k}} = j'_{\mathbf{k}} = 0\}$. We take out the diagram for $W = S^* S$, which is obtained from W above as follows. Remove the propagator (3.1), connect $\phi_{n=1;\mathbf{k}}$, Eq. (2.6), to the vertex v_1 in S , and connect $\phi_{n'=1;\mathbf{k}}$ to v_2 . Here $\phi_{n=1;\mathbf{k}}$ [$\phi_{n'=1;\mathbf{k}}$] designates that, in Eq. (2.6), $iK_{\mathbf{k},n=1}$ [$iK_{\mathbf{k},n'=1}^*$] operates on $\phi_{n=1}$ [$\phi_{n'=1}$]. We pick out, from Eq. (2.6),

$$N_{ii'}^{nn'} = N_{11}^{nn} = n. \quad (3.2)$$

Here and below, we suppress the suffix \mathbf{k} , whenever no confusion arises. In S^* , $N_{jj'}^{nn'} = N_{00}^{nn} = 1$. Inserting $N_{jj'}^{nn'}$, $N_{ii'}^{nn'} = n$ into Eq. (2.3b) with Eq. (2.3d), we obtain

$$\langle n \rangle = \frac{1}{e^{\beta p} - 1} \equiv n_B(p). \quad (3.3)$$

Here $n_B(p)$ is the Bose distribution function and the angular brackets denote the statistical average

$$\langle \Omega_n \rangle \equiv \frac{\sum_{n=0}^{\infty} e^{-\beta n p} \Omega_n}{\sum_{n=0}^{\infty} e^{-\beta n p}}.$$

Then, in \mathcal{N} in Eq. (2.3b), the portion corresponding to Eq. (3.1) turns out to

$$\frac{1}{2pV} n_B(p) = \frac{1}{V} \int_{-\infty}^{\infty} \frac{dp_0}{2\pi} \theta(p_0) 2\pi \delta(P^2) n_B(p), \quad (3.4)$$

where $1/(2pV)$ has come from $iK_{\mathbf{k},n'=1}^* iK_{\mathbf{k},n=1}$ in Eq. (2.6) with Eq. (2.8). It is to be noted that $Z_{\Phi}^{-1/2}$ in K 's, Eq. (2.8), may be dealt with just as in vacuum theory, so that we ignore $Z_{\Phi}^{-1/2}$ throughout this paper.

$\{i_{-\mathbf{k}} = i'_{-\mathbf{k}} = 1, j_{-\mathbf{k}} = j'_{-\mathbf{k}} = 0\}$. The relative diagram to the above diagram for $W = S^* S$, same as above W except that $\phi_{n=1;-\mathbf{k}}$ ($\phi_{n'=1;-\mathbf{k}}$) is connected to the vertex v_2 (v_1), yields, in place of Eq. (3.4),

$$\frac{1}{V} \int_{-\infty}^{\infty} \frac{dp_0}{2\pi} \theta(-p_0) 2\pi \delta(P^2) n_B(p). \quad (3.5)$$

Adding Eqs. (3.1), (3.4), and (3.5), we extract

$$\begin{aligned} \frac{i}{P_{\mathbf{k}}^2 + i0^+} + 2\pi n_B(p_{\mathbf{k}}) \delta(P_{\mathbf{k}}^2) & \equiv iD_{11}(P_{\mathbf{k}}) \\ & \equiv iD_{11}^{(0)}(P_{\mathbf{k}}) + iD_{11}^{(T)}(P_{\mathbf{k}}). \end{aligned} \quad (3.6)$$

Here $iD_{11}^{(0)}$ and $iD_{11}^{(T)}$ stand, respectively, for the T -independent part [the first term on the left-hand side (LHS)] and the T -dependent part (the second term) of iD_{11} .

(c) $\{i_{\mathbf{k}}=j_{\mathbf{k}}=0, i'_{\mathbf{k}}=j'_{\mathbf{k}}=1\}$ and $\{i_{-\mathbf{k}}=j_{-\mathbf{k}}=1, i'_{-\mathbf{k}}=j'_{-\mathbf{k}}=0\}$. In order to extract the contribution of $\{i_{\mathbf{k}}=j_{\mathbf{k}}=0, i'_{\mathbf{k}}=j'_{\mathbf{k}}=1\}$, we take a diagram for $W=S^*S$ in \mathcal{N} , Eq. (2.3b), where $\phi_{n'=1;\mathbf{k}}$ in S is connected to the vertex v_1 in S and $\phi_{n'=1;\mathbf{k}}$ in S^* is connected to the vertex v_2 in S^* .

We pick out from Eq. (2.6) and from the form of S^* ,

$$N_{ii'}^{nn'} N_{jj'}^{nn'} = N_{01}^{n,n+1} N_{01}^{n,n+1} = n+1.$$

Inserting into Eq. (2.3b) yields

$$1+n \rightarrow 1+n_B(p). \quad (3.7)$$

Then, in \mathcal{N} in Eq. (2.3b), the portion under consideration takes the form

$$\frac{1}{V} \int_{-\infty}^{\infty} \frac{dp_0}{2\pi} \theta(p_0) 2\pi \{1+n_B(p)\} \delta(P^2). \quad (3.8)$$

$\{i_{-\mathbf{k}}=j_{-\mathbf{k}}=1, i'_{-\mathbf{k}}=j'_{-\mathbf{k}}=0\}$. We consider the relative diagram for $W=S^*S$, which is the same as above except that $\phi_{n=1;-\mathbf{k}}$ in S is connected to the vertex v_1 and $\phi_{n=1;-\mathbf{k}}$ in S^* is connected to the vertex v_2 . In a similar manner as above, we have

$$\frac{1}{V} \int_{-\infty}^{\infty} \frac{dp_0}{2\pi} \theta(-p_0) 2\pi n_B(p) \delta(P^2). \quad (3.9)$$

Adding Eqs. (3.8) and (3.9), we extract

$$2\pi [\theta(p_{\mathbf{k}0}) + n_B(p_{\mathbf{k}})] \delta(P_{\mathbf{k}}^2) \equiv iD_{21}(P_{\mathbf{k}}). \quad (3.10)$$

(d) $\{i_{\mathbf{k}}=i'_{\mathbf{k}}=j_{\mathbf{k}}=j'_{\mathbf{k}}=0\}$, $\{i_{\mathbf{k}}=i'_{\mathbf{k}}=0, j_{\mathbf{k}}=j'_{\mathbf{k}}=1\}$, and $\{i_{-\mathbf{k}}=i'_{-\mathbf{k}}=0, j_{-\mathbf{k}}=j'_{-\mathbf{k}}=1\}$. In a similar manner as in (a) and (b) above, we extract

$$\begin{aligned} \frac{-i}{P_{\mathbf{k}}^2 - i0^+} + 2\pi n_B(p_{\mathbf{k}}) \delta(P_{\mathbf{k}}^2) &\equiv iD_{22}(P_{\mathbf{k}}) \\ &\equiv iD_{22}^{(0)}(P_{\mathbf{k}}) + iD_{22}^{(T)}(P_{\mathbf{k}}) \end{aligned} \quad (3.11)$$

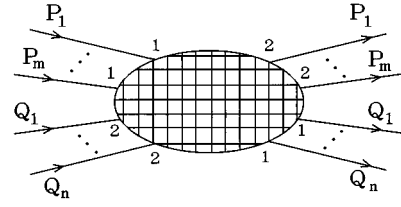


FIG. 2. Diagrammatic representation of the thermal amplitude A in Eq. (3.14).

$$= [iD_{11}(P_{\mathbf{k}})]^*.$$

(e) $\{i_{\mathbf{k}}=j_{\mathbf{k}}=1, i'_{\mathbf{k}}=j'_{\mathbf{k}}=0\}$ and $\{i_{-\mathbf{k}}=j_{-\mathbf{k}}=0, i'_{-\mathbf{k}}=j'_{-\mathbf{k}}=1\}$. In a similar manner as in (c) above, we extract

$$\begin{aligned} 2\pi [\theta(-p_{\mathbf{k}0}) + n_B(p_{\mathbf{k}})] \delta(P_{\mathbf{k}}^2) &\equiv iD_{12}(P_{\mathbf{k}}) \\ &\equiv iD_{21}(-P_{\mathbf{k}}). \end{aligned} \quad (3.12)$$

The forms of $D_{ij}(P)$ ($i, j=1, 2$) defined above are nothing but the thermal propagators in the Keldish variant of the RTF, which is defined on the time path C , $-\infty \rightarrow +\infty \rightarrow -\infty \rightarrow -\infty - i\beta$, in a complex time plane. The above derivation shows that the suffix 1 of D_{ij} stands for the vertex in S and the suffix 2 stands for the vertex in S^* . On the other hand, in the RTF, the suffix 1 stands for physical or type-1 field and 2 stands for thermal-ghost or type-2 field.

Let us turn to identify the vertex factors. We take the interaction Lagrangian density

$$\mathcal{L}_{\text{int}} = g\Phi\phi' / \ell' + \lambda\phi' / \ell'!. \quad (3.13)$$

Then, a $\Phi\phi'$ (ϕ' / ℓ') vertex in S receives the factor ig ($i\lambda$), and then a $\Phi\phi'$ (ϕ' / ℓ') vertex in S^* receives the factor $-ig$ ($-i\lambda$). This again is in accordance with the RTF, where ig ($-ig$) and $i\lambda$ ($-i\lambda$) are the factors which are associated with, in respective order, $\Phi\phi'$ and ϕ' / ℓ' vertices of type-1 (type-2) fields.

Repeating the above procedure, we finally obtain

$$\frac{1}{V} \left(\prod_{j=1}^n 2q_j V \right) \mathcal{R} = \left(\prod_{i=1}^m \frac{1}{2p_i V} \right) A(P_1^{(2)}, \dots, P_m^{(2)}, Q_1^{(1)}, \dots, Q_n^{(1)}; P_1^{(1)}, \dots, P_m^{(1)}, Q_1^{(2)}, \dots, Q_n^{(2)}). \quad (3.14)$$

Here A represents the *thermal amplitude* in the Keldish variant of the RTF for the forward process,

$$\sum_{i=1}^m \Phi_1(P_i) + \sum_{j=1}^n \Phi_2(Q_j) \rightarrow \sum_{i=1}^m \Phi_2(P_i) + \sum_{j=1}^n \Phi_1(Q_j),$$

where Φ_1 (Φ_2) is a type-1 (type-2) field. The thermal amplitude A is diagrammed in Fig. 2. As we have assumed that $W=S^*S$ represents the connected diagram [cf. above after Eq. (2.4)], the diagram for A is connected.

Each loop momentum P in A accompanies

$$\frac{1}{V} \sum_{\mathbf{P}_{\mathbf{k}}} \int \frac{dp_0}{2\pi}. \quad (3.15)$$

In the large V limit the LHS of Eq. (3.14) becomes

$$\frac{1}{V} \left(\prod_{j=1}^n 2q_j V \right) \mathcal{R} \rightarrow \frac{1}{V} \left(\prod_{j=1}^n 2E_j \frac{d}{d\mathbf{q}_j / (2\pi)^3} \right) \mathcal{R}$$

and Eq. (3.15) becomes

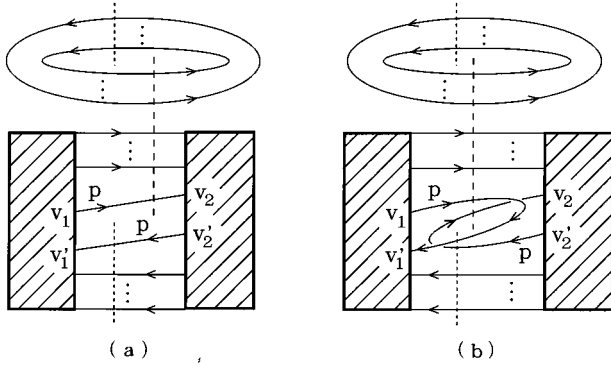


FIG. 3. Double-cut diagrams for $W=S^*S$, which yields (a) $iD_{12}^{(+)}(P)iD_{21}^{(+)}(P)$ and (b) $iD_{11}^{(T)(+)}(P)iD_{22}^{(T)(+)}(P)$. Here $P=(\mathbf{p}, p)$.

$$\frac{1}{V} \sum_{\mathbf{pk}} \int \frac{dp_0}{2\pi} \rightarrow \int \frac{d^4P}{(2\pi)^4}. \quad (3.16)$$

So far, \mathcal{D} in Eq. (2.3c) does not participate; $\mathcal{D}=1$ [cf. Eq. (2.4)]. The role of \mathcal{D} will be discussed below.

B. Analysis of mode-overlapping diagrams, $i_{\mathbf{k}}+i'_{\mathbf{k}}+j_{\mathbf{k}}+j'_{\mathbf{k}} \geq 4$

The above derivation of the thermal reaction-rate formula is not complete in that we have only considered the cases where $i_{\mathbf{k}}+i'_{\mathbf{k}}+j_{\mathbf{k}}+j'_{\mathbf{k}} \leq 2$. When generalized self-energy parts are involved in $W=S^*S$, $i_{\mathbf{k}}+i'_{\mathbf{k}}+j_{\mathbf{k}}+j'_{\mathbf{k}} \geq 4$. (We call the diagram with $i_{\mathbf{k}}+i'_{\mathbf{k}}+j_{\mathbf{k}}+j'_{\mathbf{k}} \geq 4$ the mode-overlapping diagram.) As mentioned in Sec. I, a complete analysis of the classes of diagrams that leads to RTF diagrams including thermal propagators with n (≥ 2) thermal self-energy insertions is still lacking. In this subsection, dealing with mode-overlapping diagrams, we shall complete the derivation of the thermal reaction-rate formula. We shall show at the same time that there is no finite-volume correction to the formula.

For illustration of the procedure, we start with analyzing the diagram (for $W=S^*S$) with $\{i_{\mathbf{k}}=j_{\mathbf{k}}=i'_{\mathbf{k}}=j'_{\mathbf{k}}=1\}$. Let us focus our attention on ϕ with mode \mathbf{k} . Both in S and in S^* , there are one ‘‘absorber vertex’’ (v'_1 and v_2 in Fig. 3) and one ‘‘emitter vertex’’ (v_1 and v'_2 in Fig. 3).

From S^*S , pick out the factor

$$N_{11}^{nn'} N_{11}^{nn'} = n^2,$$

where and below the suffix ‘‘ \mathbf{k} ’’ is dropped whenever no confusion arises. In \mathcal{N} in Eq. (2.3b), we have, in place of Eq. (3.3),

$$\begin{aligned} \langle n^2 \rangle &= 2n_B^2 + n_B \\ &= n_B(1+n_B) + n_B^2, \end{aligned} \quad (3.17)$$

where $n_B \equiv n_B(p)$.

The first term on the right-hand side (RHS) of Eq. (3.17) goes to

$$\begin{aligned} \{2\pi\theta(p_0)n_B(p)\delta(P^2)\}\{2\pi\theta(p_0)[1+n_B(p)]\delta(P^2)\} \\ = iD_{12}^{(+)}(P)iD_{21}^{(+)}(P), \end{aligned} \quad (3.18)$$

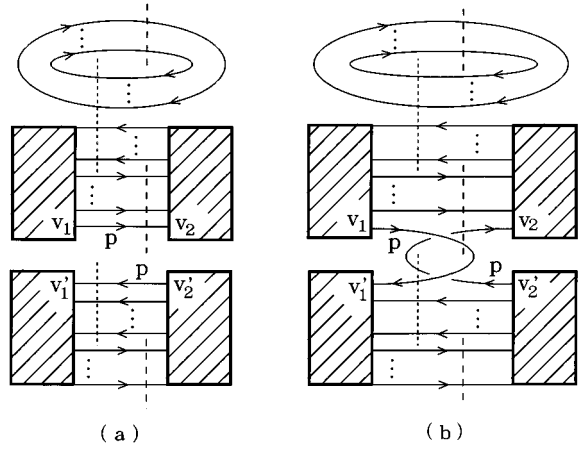


FIG. 4. Double-cut diagrams for $W=S^*S$, which yields (a) $iD_{12}^{(+)}(P)iD_{21}^{(+)}(P)$ and (b) $iD_{11}^{(T)(+)}(P)iD_{22}^{(T)(+)}(P)$. Here $P=(\mathbf{p}, p)$.

where $D_{12/21}^{(\pm)}(P) \equiv \theta(\pm p_0)D_{12/21}(P)$. The (part of) thermal propagator $iD_{12}^{(+)}(P)$ [$iD_{21}^{(+)}(P)$] is diagrammed in the double-cut diagram for $W=S^*S$, Fig. 3(a), as the line that connects the emitter vertex v'_2 (v_1) with the absorber vertex v'_1 (v_2).

The second term of Eq. (3.17) goes to

$$[2\pi\theta(p_0)n_B(E)\delta(P^2)]^2 = iD_{11}^{(T)(+)}(P)iD_{22}^{(T)(+)}(P). \quad (3.19)$$

$iD_{11}^{(T)(+)}(P)$ ($iD_{22}^{(T)(+)}(P)$) is diagrammed in the double-cut diagram, Fig. 3(b), as the line that connects the emitter vertex v_1 (v'_2) with the absorber vertex v'_1 (v_2). Thus, with obvious notation, the $n_B(1+n_B)$ part in Eq. (3.17) ‘‘supplies’’ the $(++)$ portion of $iD_{12}(P)iD_{21}(P)$, Fig. 3(a), and the n_B^2 part ‘‘supplies’’ the $(++)$ part of $iD_{11}^{(T)}(P)iD_{22}^{(T)}(P)$ in Fig. 3(b).

The $(--)$ portion of $iD_{12}(P)iD_{21}(P)$ emerges from $W=S^*S$, which is the same as Fig. 3 except that $\{i_{-\mathbf{k}}=j_{-\mathbf{k}}=i'_{-\mathbf{k}}=j'_{-\mathbf{k}}=1\}$. Now, v_1 and v'_2 (v'_1 and v_2) are absorber (emitter) vertices. The $(+,-)$ portion comes from $W=S^*S$ with $\{i_{\mathbf{k}}=i_{-\mathbf{k}}=j_{\mathbf{k}}=j_{-\mathbf{k}}=1\}$. This time, v_1 and v'_1 (v_2 and v'_2) are absorber (emitter) vertices. The $(-+)$ portion comes from $W=S^*S$ with $\{i'_{\mathbf{k}}=i'_{-\mathbf{k}}=j'_{\mathbf{k}}=j'_{-\mathbf{k}}=1\}$, where the absorber (emitter) vertices are v_2 and v'_2 (v_1 and v'_1). Adding all these contributions to the contribution (3.18), we obtain Eq. (3.18) with complete $iD_{12}(P)iD_{21}(P)$. In a similar manner, we can find a set of relative diagrams, which, together with Eq. (3.19), yield the complete $iD_{11}(P)iD_{22}(P)$.

All the vertices v_1 , v'_1 , v_2 , and v'_2 (cf. Fig. 3) are not necessarily within one connected diagram. There is a diagram as depicted, e.g., in Fig. 4. Figure 4(a) [4(b)] contains the factor $iD_{12}^{(+)}iD_{21}^{(+)}$ [$iD_{11}^{(T)(+)}iD_{22}^{(T)(+)}$] in Eq. (3.18) [Eq. (3.19)]. Let us inspect Fig. 4(a). As stated above after Eq. (2.4), we are considering the case where $\{A, B\}_S$ and $\{A, B\}_{S^*}$ [$\{A\}=\{\Phi(P_i)\}$ and $\{B\}=\{\Phi(Q_j)\}$] are involved in one connected part of $W=S^*S$. Then, all Φ 's are in, e.g., the bottom subdiagram in Fig. 4(a) [and then also in Fig. 4(b)] and, in the middle subdiagram, only constituent particles ϕ 's

of the heat bath participate. $iD_{21}^{(+)}(P)$ is involved in the middle subdiagram, which goes to \mathcal{D} , while $iD_{12}^{(+)}(P)$ is involved in the bottom subdiagram, which goes to \mathcal{N}_{con} . Thus, Fig. 4(a) is in $\mathcal{N}_{con}\mathcal{D}$ with $\mathcal{D} \neq 1$ in Eq. (2.5) with Eq. (2.4). As a matter of fact, \mathcal{N}_{con} here is obtained from $W = S^*S$ with $\{i_{\mathbf{k}} = j_{\mathbf{k}} = 1, i'_{\mathbf{k}} = j'_{\mathbf{k}} = 0\}$ and \mathcal{D} is obtained from $W_0 = S_0^*S_0$ [cf. Eq. (2.3c)] with $\{i_{\mathbf{k}} = j_{\mathbf{k}} = 0, i'_{\mathbf{k}} = j'_{\mathbf{k}} = 1\}$. Thus, Fig. 4(a) does contribute to \mathcal{R} in Eq. (2.3a) as $\mathcal{R} = \mathcal{N}_{con}$, which already appears at lower order of the perturbation series. As above, it is straightforward to find a set of relative diagrams, which, together with Fig. 4(a), yields the complete $iD_{12}(P)iD_{21}(P)$. Similarly one can find a set of relative diagrams, which, together with Fig. 4(b), yields the complete $iD_{11}(P)iD_{22}(P)$.

The relevant part of Fig. 4(b) and its ‘‘relatives’’ sits in A , Eq. (3.14), as a (1,2) component of a thermal self-energy-inserted propagator. Thus, $W = S^*S$ with $\{i_{\mathbf{k}} = j_{\mathbf{k}} = i'_{\mathbf{k}} = j'_{\mathbf{k}} = 1\}$ together with its ‘‘relatives’’ has turned out to take the proper seat in A in Eq. (3.14).

It is straightforward to generalize the above argument to a generic diagram for $W = S^*S$. Let us focus our attention on a mode \mathbf{k} . We analyze \mathcal{N} in Eq. (2.3b). Let $\phi_{\mathbf{k}}$ be ϕ in the mode \mathbf{k} . In S in Eq. (2.6), $i_{\mathbf{k}}$ $\phi_{\mathbf{k}}$'s in the initial state and $i'_{\mathbf{k}}$ $\phi_{\mathbf{k}}$'s in the final state participate directly in the reaction. In S^* , $j_{\mathbf{k}}$ ($j'_{\mathbf{k}}$) $\phi_{\mathbf{k}}$'s in the initial (final) state participate directly; $i_{\mathbf{k}} - i'_{\mathbf{k}} = j_{\mathbf{k}} - j'_{\mathbf{k}} = n_{\mathbf{k}} - n'_{\mathbf{k}}$. In S , there are $i_{\mathbf{k}}$ ($i'_{\mathbf{k}}$) ‘‘absorber vertices’’ (‘‘emitter vertices’’) and, in S^* , there are $j_{\mathbf{k}}$ ($j'_{\mathbf{k}}$) ‘‘emitter vertices’’ (‘‘absorber vertices’’). (Recall that, in the case of Figs. 3 and 4, v'_1 and v_2 are absorber vertices and v_1 and v'_2 are emitter vertices.)

We pick out, from $W = S^*S$,

$$\begin{aligned} N_{jj'}^{nn'} N_{ii'}^{nn'} &= \frac{n!n'!}{(n-i)!(n-j)!} \frac{1}{i!i'!j!j'!} \\ &= \frac{1}{i!i'!j!j'!} \prod_{k=0}^{i'-1} (n+i'-i-k) \prod_{k=0}^{j-1} (n-k), \end{aligned} \quad (3.20)$$

where and below the suffix \mathbf{k} has been dropped. From the

form for S , Eq. (2.6), we see that the permutation of $\phi_{n'}$ ($n' = 1, \dots, i'_{\mathbf{k}}$) and the permutation of ϕ_n ($n = 1, \dots, i_{\mathbf{k}}$) give the same diagram, and then $i_{\mathbf{k}}!i'_{\mathbf{k}}!$ same diagrams emerge. Then $i_{\mathbf{k}}!i'_{\mathbf{k}}!j_{\mathbf{k}}!j'_{\mathbf{k}}!$ same diagrams emerge for $W = S^*S$, which eliminates the first factor on the RHS of Eq. (3.20). In \mathcal{N} in Eq. (2.3b), we have, in place of Eq. (3.3),

$$\left\langle \prod_{k=0}^{i'-1} (n+i'-i-k) \prod_{k=0}^{j-1} (n-k) \right\rangle \equiv H_{j,j'}^{i,i'}.$$

Here it is convenient to introduce a generating function of $H_{j,j'}^{i,i'}$,

$$f(y,z) \equiv \sum_{n=0}^{\infty} y^{n+i'-i} z^n e^{-xn} \quad (x = \beta p = \beta p_{\mathbf{k}}). \quad (3.21)$$

In fact, from Eq. (3.21), we obtain

$$H_{j,j'}^{i,i'} = \frac{1}{f} \frac{\partial^2 f}{\partial y^{i'} \partial x^j} \Big|_{y=z=1}. \quad (3.22)$$

From Eq. (3.22) with Eq. (3.21), it can be shown that

$$H_{j,j'}^{i,i'} = \sum_{k=0}^{\min(i',j')} \binom{i'}{k} \frac{j'!(j+i'-k)!}{(j'-k)!} \{n_B(x)\}^{j+i'-k}. \quad (3.23)$$

Since $i - i' = j - j'$, we can readily see that $H_{j,j'}^{i,i'}$, Eq. (3.23), is symmetric under $(i, i') \leftrightarrow (j, j')$. Then, without loss of generality, we assume $i \geq j$.

In the Appendix, we show that

$$H_{j,j'}^{i,i'} = \sum_{k=0}^{\min(j,j')} \frac{i!}{(i-j+k)!} \frac{i'!j'!}{(j'-k)!} \binom{j}{k} (n_B)^{i+k} (1+n_B)^{j'-k} \quad (3.24)$$

$$= \sum_{k=0}^{\min(j,j')} \{C_{i,j}^k (n_B)^{j-k}\} \{C_{i',i-j+k}^0 (n_B)^{i-j+k}\} \{C_{j',k}^0 (n_B)^k\} \{C_{j'-k,j'-k}^0 (1+n_B)^{j'-k}\}. \quad (3.25)$$

Here $n_B \equiv n_B(p)$ and

$$C_{i,j}^k \equiv \frac{i!}{(i-j+k)!} \binom{j}{k}.$$

In Eq. (3.25), the factor $C_{i,j}^k$ may be identified as the number of ways of connecting $j-k$ (out of j) emitter vertices in S^*

to i absorber vertices in S , the factor $C_{i',i-j+k}^0$ to the number of ways of connecting $i-j+k$ absorber vertices in S to i' emitter vertices in S , the factor $C_{j',k}^0$ to the number of ways of connecting k emitter vertices in S^* to j' absorber vertices in S^* , and the factor $C_{j'-k,j'-k}^0$ to the number of ways of connecting $j'-k$ absorber vertices in S^* to $i' - (i - j + k)$

$= j' - k$ emitter vertices in S . Then, in \mathcal{R} in Eqs. (2.3a), we have, in place of Eqs. (3.18) and (3.19),

$$\begin{aligned} & \sum_{k=0}^{\min(j,j')} [C_{i,j}^k \{iD_{12}^{(+)}(p)\}^{j-k}] [C_{i',i-j+k}^0 \{iD_{11}^{(T)(+)}(p)\}^{i-j+k}] \\ & \times [C_{j',k}^0 \{iD_{22}^{(T)(+)}(p)\}^k] [C_{j'-k,j'-k}^0 \{iD_{21}^{(+)}(p)\}^{j'-k}]. \end{aligned} \quad (3.26)$$

This is just a portion of ‘‘right’’ thermal amplitude in the RTF. Just as in the simple case $\{i_{\mathbf{k}}=j_{\mathbf{k}}=i'_{\mathbf{k}}=j'_{\mathbf{k}}=1\}$, analyzed above, we can find a set of relative diagrams for $W=S^*S$, which, together with Eq. (3.26), leads to Eq. (3.26) with complete D 's. Among the diagrams that accompany Eq. (3.26) with complete D 's, are disconnected ones like Fig. 4(a). Such diagrams belong to $\mathcal{N}=\mathcal{N}_{con}\mathcal{D}$ with $\mathcal{D}\neq 1$ [cf. Eq. (2.5)], and then do contribute to \mathcal{R} in Eq. (2.3a) as $\mathcal{R}=\mathcal{N}_{con}$. Connected diagrams that accompany Eq. (3.26) with complete D 's take the proper seat in A in Eq. (3.14).

Conversely, for any diagram for A in Eq. (3.14), through the analysis running in the opposite direction, one can identify a set of diagrams for $W=S^*S$. The analysis made above is so general that no additional comment is necessary on the diagrams that lead to A , Eq. (3.14), which includes thermal propagator(s) with n (≥ 2) thermal self-energy insertion.

This completes the derivation of the formula (3.14) for the rate of a generic thermal reaction taking place in a heat bath of finite volume. Keeping in mind a suitable normalization for incident fluxes of Φ 's, the formula (3.14) ‘‘smoothly’’ goes to the formula for the infinite-volume ($V=\infty$) system [cf. Eq. (3.16)] in the sense that there do not exist extra contributions in Eq. (3.14) with $V<\infty$, which disappear in the limit $V\rightarrow\infty$. Thus, there is no finite-volume correction to the thermal reaction-rate formula (3.14).

Here we make a comment on gauge theories. Choosing a physical gauge like the Coulomb gauge, the gauge boson may be dealt with in a similar manner to the above scalar-field case. When we adopt a covariant gauge, a Faddeev-Popov (FP) ghost field comes on the stage. The first summations in Eqs. (2.3b) and (2.3c) are carried out over the modes of physical degrees of freedom. This can be implemented by inserting the projection operator \mathcal{P} onto the physical space on the left side of ρ in Eqs. (2.3b) and (2.3c) and the sum is taken over $\{n_{\mathbf{k}}^{(\alpha)}\}$ for all, unphysical as well as physical, modes α 's. As far as the ensemble average of physical quantities like the reaction rate are concerned, the entire role of \mathcal{P} is to make [19] the antiperiodic boundary condition for FP ghost field the periodic one, $\phi_{FP}(t-i\beta, \mathbf{x}) = \phi_{FP}(t, \mathbf{x})$, so that the bare FP ghost propagator is the same in form to the scalar propagator. Keeping this fact in mind, we can deduce Eq. (3.14), where A is evaluated using standard gauge-field and FP ghost thermal propagators in the covariant gauge.

IV. DIRAC FERMION

We study the case of the Dirac fermion. The expression for S in Eq. (2.6) with Eqs. (2.7) and (2.8) is changed accordingly. Let $n_{\mathbf{k}}^{(\sigma)}$ [$\bar{n}_{\mathbf{k}}^{(\sigma)}$] ($\sigma=\pm$) be the number of mode- \mathbf{k} fermion [antifermion] with helicity σ . The combinatorial

factor $N_{i_{\mathbf{k}}i'_{\mathbf{k}}}^{n_{\mathbf{k}}n'_{\mathbf{k}}}$ in Eq. (2.6) is changed to

$$\begin{aligned} N_f &= \prod_{\sigma=\pm} \left(N_{i_{\mathbf{k}}i'_{\mathbf{k}}}^{n_{\mathbf{k}}^{(\sigma)}n_{\mathbf{k}}^{(\sigma)'}} N_{\bar{i}_{\mathbf{k}}\bar{i}'_{\mathbf{k}}}^{\bar{n}_{\mathbf{k}}^{(\sigma)}\bar{n}_{\mathbf{k}}^{(\sigma)'}} \right) \\ &\equiv \prod_{\sigma=\pm} \left[\begin{pmatrix} n_{\mathbf{k}}^{(\sigma')} \\ i_{\mathbf{k}}^{(\sigma')} \end{pmatrix} \begin{pmatrix} n_{\mathbf{k}}^{(\sigma)} \\ i_{\mathbf{k}}^{(\sigma)} \end{pmatrix} \begin{pmatrix} \bar{n}_{\mathbf{k}}^{(\sigma')} \\ \bar{i}_{\mathbf{k}}^{(\sigma')} \end{pmatrix} \begin{pmatrix} \bar{n}_{\mathbf{k}}^{(\sigma)} \\ \bar{i}_{\mathbf{k}}^{(\sigma)} \end{pmatrix} \right], \end{aligned} \quad (4.1)$$

where $n_{\mathbf{k}}^{(\sigma)} - i_{\mathbf{k}}^{(\sigma)} = n_{\mathbf{k}}^{(\sigma')} - i_{\mathbf{k}}^{(\sigma)'}$ and $\bar{n}_{\mathbf{k}}^{(\sigma)} - \bar{i}_{\mathbf{k}}^{(\sigma)} = \bar{n}_{\mathbf{k}}^{(\sigma')} - \bar{i}_{\mathbf{k}}^{(\sigma)'}$. In Eqs. (2.3b) and (2.3c), the summations on $n_{\mathbf{k}}^{(\sigma)}$, $n_{\mathbf{k}}^{(\sigma)'}$, $\bar{n}_{\mathbf{k}}^{(\sigma)}$, and $\bar{n}_{\mathbf{k}}^{(\sigma)'}$ are taken over 0 and 1. We assume that the interaction Lagrangian is bilinear in fermion fields, which include fermion fields constituting the heat bath and possibly nonthermalized heavy fermion fields, the counterpart of Φ 's in Eq. (2.6).

A. Analysis of non-mode-overlapping diagrams

We proceed as in Sec. III A using the same notation.

(a) $\{i_{\mathbf{k}}^{(\sigma)}=i_{\mathbf{k}}^{(\sigma)'}=j_{\mathbf{k}}^{(\sigma)}=j_{\mathbf{k}}^{(\sigma)'}=\bar{i}_{\mathbf{k}}^{(\sigma)}=\bar{i}_{\mathbf{k}}^{(\sigma)'}=\bar{j}_{\mathbf{k}}^{(\sigma)}=\bar{j}_{\mathbf{k}}^{(\sigma)'}=0\}$ ($\sigma=\pm$). In place of Eq. (3.1), we have

$$\frac{1}{V} \int_{-\infty}^{\infty} \frac{dp_0}{2\pi} \frac{i\mathcal{P}}{p^2+i0^+}, \quad (4.2)$$

which comes from the following contraction in S [cf. Eq. (2.6)]:

$$\begin{aligned} & \langle 0 | T [\cdots \overbrace{\bar{\psi}(x_1)\psi(x_1)\cdots\bar{\psi}(x_2)\psi(x_2)\cdots} | 0 \rangle \\ & = iS_F(x_1-x_2) \langle 0 | T [\cdots \bar{\psi}(x_1)\cdots\psi(x_2)\cdots] | 0 \rangle. \end{aligned} \quad (4.3)$$

Here $\bar{\psi}\psi$'s in Eq. (4.3) come from the interaction Lagrangian \mathcal{L}_{int} .

(b) Fermion mode with $\{i_{\mathbf{k}}^{(\sigma)}=i_{\mathbf{k}}^{(\sigma)'}=1, j_{\mathbf{k}}^{(\sigma)}=j_{\mathbf{k}}^{(\sigma)'}=0\}$ ($\sigma=\pm$) and its relative. We consider the positive-helicity ($\sigma=+$) fermion mode with $\{i_{\mathbf{k}}^{(+)}=i_{\mathbf{k}}^{(+)'}=1, j_{\mathbf{k}}^{(+)}=j_{\mathbf{k}}^{(+)'}=0\}$. In place of Eqs. (3.2) and (3.3), we have, in respective order,

$$N_f = n^2$$

and

$$\langle n^2 \rangle = \frac{1}{e^{\beta p} + 1} \equiv n_F(p),$$

where $n_F(p)$ is the Fermi distribution function and $\langle \Omega_n \rangle \equiv \sum_{n=0}^1 e^{-\beta n p} \Omega_n / \sum_{n=0}^1 e^{-\beta n p}$. We note that the contribution corresponding to Eq. (4.3) above is [cf. Eq. (2.6)]

$$\begin{aligned} & \langle 0 | T [\cdots \overbrace{\psi_{n'=1}(y) \bar{\psi}(x_1) \psi(x_1) \cdots \bar{\psi}(x_2) \psi(x_2) \bar{\psi}_{n=1}(z) \cdots}] | 0 \rangle \\ & = -iS_F(y-x_2) iS_F(x_1-z) \langle 0 | T [\cdots \bar{\psi}(x_1) \cdots \psi(x_2) \cdots] | 0 \rangle. \end{aligned}$$

Then, the LHS of Eq. (3.4) is replaced by

$$-\frac{1}{2pV} n_F(p) u^{(+)}(P) \bar{u}^{(+)}(P).$$

Adding the contribution from the negative-helicity fermion mode with $\{i_{\mathbf{k}}^{(-)} = i_{\mathbf{k}}^{(-)'} = 1, j_{\mathbf{k}}^{(-)} = j_{\mathbf{k}}^{(-)'} = 0\}$, we have

$$\begin{aligned} & -\frac{1}{2pV} n_F(p) \sum_{\sigma=\pm} u^{(\sigma)}(P) \bar{u}^{(\sigma)}(P) \\ & = -\frac{1}{V} \int_{-\infty}^{\infty} \frac{dp_0}{2\pi} \theta(p_0) 2\pi \delta(P^2) n_F(p) \mathcal{P}. \quad (4.4) \end{aligned}$$

Adding further the contribution from the antifermion modes with $\{\bar{i}_{-\mathbf{k}}^{(\sigma)} = \bar{i}_{-\mathbf{k}}^{(\sigma)'} = 1, \bar{j}_{-\mathbf{k}}^{(\sigma)} = \bar{j}_{-\mathbf{k}}^{(\sigma)'} = 0\}$ ($\sigma = \pm$) to Eqs. (4.2) and (4.4), we extract

$$\begin{aligned} & \left[\frac{i}{P_{\mathbf{k}}^2 + i0^+} - 2\pi n_F(p_{\mathbf{k}}) \delta(P_{\mathbf{k}}^2) \right] \mathcal{P}_{\mathbf{k}} \\ & \equiv iS_{11}(P_{\mathbf{k}}) = iS_{11}^{(0)}(P_{\mathbf{k}}) + iS_{11}^{(T)}(P_{\mathbf{k}}). \quad (4.5) \end{aligned}$$

(c) Fermion mode with $\{i_{\mathbf{k}}^{(\sigma)} = j_{\mathbf{k}}^{(\sigma)} = 0, i_{\mathbf{k}}^{(\sigma)'} = j_{\mathbf{k}}^{(\sigma)'} = 1\}$ ($\sigma = \pm$) and its relative. In place of Eq. (3.7), we have

$$1 - n_F(p).$$

Then, Eq. (3.8) is replaced by

$$\frac{1}{V} \int_{-\infty}^{\infty} \frac{dp_0}{2\pi} \theta(p_0) 2\pi \{1 - n_F(p)\} \delta(P^2) \mathcal{P}.$$

Adding the contribution from the antifermion mode with $\{\bar{i}_{-\mathbf{k}}^{(\sigma)} = \bar{j}_{-\mathbf{k}}^{(\sigma)} = 1, \bar{i}_{-\mathbf{k}}^{(\sigma)'} = \bar{j}_{-\mathbf{k}}^{(\sigma)'} = 0\}$ ($\sigma = \pm$), we extract

$$2\pi [\theta(p_0) - n_F(p_{\mathbf{k}})] \delta(P_{\mathbf{k}}^2) \mathcal{P}_{\mathbf{k}} \equiv iS_{21}(P_{\mathbf{k}}).$$

(d) Interchanging the roles of S and S^* in (a) and (b) above, we obtain, in place of Eq. (3.11),

$$\begin{aligned} & \left[\frac{-i}{P_{\mathbf{k}}^2 - i0^+} - 2\pi n_F(p_{\mathbf{k}}) \delta(P_{\mathbf{k}}^2) \right] \mathcal{P}_{\mathbf{k}} \\ & \equiv iS_{22}(P_{\mathbf{k}}) = iS_{22}^{(0)}(P_{\mathbf{k}}) + iS_{22}^{(T)}(P_{\mathbf{k}}). \end{aligned}$$

(e) Fermion mode with $\{i_{\mathbf{k}}^{(\sigma)} = j_{\mathbf{k}}^{(\sigma)} = 1, i_{\mathbf{k}}^{(\sigma)'} = j_{\mathbf{k}}^{(\sigma)'} = 0\}$ ($\sigma = \pm$) and its relative. The relevant statistical factor is $n_F(p)$. Let us show that the part under consideration turns out to $iS_{12}(P_{\mathbf{k}})$. In place of $p_0 > 0$ portion of Eq. (3.12), we have $2\pi n_F(p_{\mathbf{k}}) \delta(P_{\mathbf{k}}^2) \mathcal{P}_{\mathbf{k}}$ which seems to be the $p_0 > 0$ portion of $iS_{12}(P_{\mathbf{k}})$. However, this is not the case. Within the resultant reaction-rate formula, which is an amplitude in the

RTF, the above factor $2\pi n_F(p_{\mathbf{k}}) \delta(P_{\mathbf{k}}^2) \mathcal{P}_{\mathbf{k}}$ necessarily appears in association with a thermal fermion loop (see below for details). The thermal fermion loop carries an extra minus sign, so that we have, for the portion under consideration,

$$iS_{12}^{(+)}(P_{\mathbf{k}}) = 2\pi [-n_F(p_{\mathbf{k}})] \delta(P_{\mathbf{k}}^2) \mathcal{P}_{\mathbf{k}}.$$

Adding the contribution from the antifermion mode with $\{\bar{i}_{-\mathbf{k}}^{(\sigma)} = \bar{j}_{-\mathbf{k}}^{(\sigma)} = 0, \bar{i}_{-\mathbf{k}}^{(\sigma)'} = \bar{j}_{-\mathbf{k}}^{(\sigma)'} = 1\}$ ($\sigma = \pm$), we extract

$$2\pi [\theta(-p_0) - n_F(p_{\mathbf{k}})] \mathcal{P}_{\mathbf{k}} \delta(P_{\mathbf{k}}^2) \equiv iS_{12}(P_{\mathbf{k}}). \quad (4.6)$$

In the process of deduction, iS_{jl} ($j, l = 1, 2$) appears in succession. At the final stage, sets of $\langle W \rangle = \langle S^* S \rangle$ turn out to be thermal amplitudes A 's [cf. Eq. (3.14)], which includes thermal loops of the fermion ψ . Out of A 's, we take a ‘‘standard’’ A_s : Each fermion loop contains at most one iS_{12} . (Note that the number of iS_{21} in a fermion loop is equal to the number of iS_{12} .) From A_s , we take two fermion loops L_1 and L_2 and let $iS_{21}(P) \in L_1$ and $iS_{21}(Q) \in L_2$. $iS_{21}(P) iS_{21}(Q)$ comes, with obvious notation, from $S^* S = S^*(\mathbf{p}, \mathbf{q}, \dots) S(\mathbf{p}, \mathbf{q}, \dots) \equiv W_s$, where S is the S -matrix element obtained using Feynman rules (in vacuum theory). The S -matrix element which is related to $S(\mathbf{p}, \mathbf{q}, \dots)$ through exchange $\mathbf{p} \leftrightarrow \mathbf{q}$ is $-S(\mathbf{q}, \mathbf{p}, \dots)$, where $S(\mathbf{q}, \mathbf{p}, \dots)$ is obtained using Feynman rules. Then, we have

$$W_s \rightarrow W = -S^*(\mathbf{p}, \mathbf{q}, \dots) S(\mathbf{q}, \mathbf{p}, \dots), \quad (4.7)$$

which brings an extra minus sign into the corresponding thermal amplitude A . Observe here that, through the above replacement of S , L_1 and L_2 in A_s turn out to be a one thermal fermion loop L in A . A thermal fermion loop carries a minus sign. Then L_1 and L_2 in A_s carries $+ = (-)^2$ while L in A carries $-$. In reducing $\langle W \rangle$ to A , the extra minus sign in Eq. (4.7) eliminates one $-$, being present in A_s , and is left with one $-$, which is interpreted as the minus sign associated with L in A . What we have shown is that A is a ‘‘right thermal amplitude.’’

Repeating the above procedure for ‘‘parent’’ A_s 's and ‘‘children’’ A 's, as ‘‘constructed’’ above, we can exhaust all A 's that contributes to the reaction-rate formula, and see that they are ‘‘right’’ thermal amplitudes.

B. Analysis of mode-overlapping diagrams

Let us turn to analyze the mode-overlapping diagrams. Noting that $n_{\mathbf{k}}^{(\sigma)}$, etc., and then also $i_{\mathbf{k}}^{(\sigma)}$, etc., take two values 0 and 1, we shall exhaust all the mode-overlapping configurations.

(a) $\{i_{\mathbf{k}}^{(\sigma)} = i_{\mathbf{k}}^{(\sigma)'} = j_{\mathbf{k}}^{(\sigma)} = j_{\mathbf{k}}^{(\sigma)'} = 1\}$ ($\sigma = \pm$) and its relatives. From Eq. (4.1), $N_f = (n^{(\sigma)})^4$ ($\sigma = \pm$), which leads to $\langle (n^{(\sigma)})^4 \rangle = n_F$. Through by now familiar manner, we extract

$$n_F \sum_{\sigma=\pm} [\{2\pi\theta(p_0)u_j^{(\sigma)}(P)\bar{u}_{j'}^{(\sigma)}(P)\} \\ \times \{2\pi\theta(p_0)u_i^{(\sigma)}(P)\bar{u}_{i'}^{(\sigma)}(P)\}], \quad (4.8)$$

$u_i^{(\sigma)}$ and $\bar{u}_{i'}^{(\sigma)}$ [$u_j^{(\sigma)}$ and $\bar{u}_{j'}^{(\sigma)}$] in Eq. (4.8) are attached to the vertices in S [S^*].

The relatives, to be analyzed, of the above configuration are $\{i_{\mathbf{k}}^{(\sigma)}=i_{\mathbf{k}}^{(\sigma)'}=j_{\mathbf{k}}^{(-\sigma)}=j_{\mathbf{k}}^{(-\sigma)'}=1\}$ and $\{i_{\mathbf{k}}^{(\sigma)}=i_{\mathbf{k}}^{(-\sigma)'}=j_{\mathbf{k}}^{(\sigma)}=j_{\mathbf{k}}^{(\sigma)'}=1\}$ ($\sigma=\pm$). The former yields

$$n_F^2 \sum_{\sigma=\pm} [\{2\pi\theta(p_0)u_j^{(-\sigma)}(P)\bar{u}_{j'}^{(-\sigma)}(P)\} \\ \times \{2\pi\theta(p_0)u_i^{(\sigma)}(P)\bar{u}_{i'}^{(\sigma)}(P)\}], \quad (4.9)$$

and the latter yields

$$n_F(1-n_F) \sum_{\sigma=\pm} [\{2\pi\theta(p_0)u_j^{(-\sigma)}(P)\bar{u}_{j'}^{(\sigma)}(P)\} \\ \times \{2\pi\theta(p_0)u_i^{(\sigma)}(P)\bar{u}_{i'}^{(-\sigma)}(P)\}]. \quad (4.10)$$

Adding Eqs. (4.8) and (4.9), we obtain

$$(iS_{22}^{(T)(+)}(P))_{jj'}(iS_{11}^{(T)(+)}(P))_{ii'} \\ + n_F(1-n_F) \sum_{\sigma=\pm} [\{2\pi\theta(p_0)u_j^{(\sigma)}(P)\bar{u}_{j'}^{(\sigma)}(P)\} \\ \times \{2\pi\theta(p_0)u_i^{(\sigma)}(P)\bar{u}_{i'}^{(\sigma)}(P)\}]. \quad (4.11)$$

Adding Eqs. (4.10) and (4.11), we have

$$(iS_{22}^{(T)(+)}(P_{\mathbf{k}}))_{jj'}(iS_{11}^{(T)(+)}(P_{\mathbf{k}}))_{ii'} \\ - (iS_{12}^{(+)}(P_{\mathbf{k}}))_{ij'}(iS_{21}^{(+)}(P_{\mathbf{k}}))_{j'i}. \quad (4.12)$$

Recalling the fact that i and i' (j and j') attach to the vertices in S (S^*), we see that Eq. (4.12) is just a portion of ‘‘right’’ thermal amplitude in the RTF. Adding an appropriate sets of relative diagrams, we can extract Eq. (4.12) with complete S 's.

(b) $\{i_{\mathbf{k}}^{(+)}=i_{\mathbf{k}}^{(-)}=j_{\mathbf{k}}^{(+)}=j_{\mathbf{k}}^{(-)}=1\}$ and its relatives. Taking care of the anticommutativity of fermion fields, we extract

$$n_F^2 [2\pi\theta(p_0)\{u_{i_1}^{(+)}(P)u_{i_2}^{(-)}(P)-u_{i_2}^{(+)}(P)u_{i_1}^{(-)}(P)\}] \\ \times [2\pi\theta(p_0)\{\bar{u}_{j_1}^{(+)}(P)\bar{u}_{j_2}^{(-)}(P)-\bar{u}_{j_2}^{(+)}(P)\bar{u}_{j_1}^{(-)}(P)\}]. \quad (4.13)$$

Here u_i 's (\bar{u}_j 's) are attached to the vertices in S (S^*). Simple manipulation yields

$$\text{Eq. (4.13)} = (iS_{12}^{(+)}(P_{\mathbf{k}}))_{i_1j_1}(iS_{12}^{(+)}(P_{\mathbf{k}}))_{i_2j_2} \\ - (iS_{12}^{(+)}(P_{\mathbf{k}}))_{i_1j_2}(iS_{12}^{(+)}(P_{\mathbf{k}}))_{i_2j_1}. \quad (4.14)$$

Adding appropriate relative diagrams, we can extract Eq. (4.14) with complete S 's, which sits on the ‘‘right seat’’ in thermal amplitude in the RTF [cf. Eq. (3.14)].

(c) $\{i_{\mathbf{k}}^{(+)}=i_{\mathbf{k}}^{(-)}=j_{\mathbf{k}}^{(+)}=j_{\mathbf{k}}^{(-)}=1, i_{\mathbf{k}}^{(\sigma)'}=j_{\mathbf{k}}^{(\sigma)'}=1\}$ ($\sigma=\pm$) and its relatives. We extract

$$n_F^2 [2\pi\theta(p_0)\{u_{i_1}^{(+)}(P)u_{i_2}^{(-)}(P)-u_{i_2}^{(+)}(P)u_{i_1}^{(-)}(P)\}] \\ \times [2\pi\theta(p_0)\{\bar{u}_{j_1}^{(+)}(P)\bar{u}_{j_2}^{(-)}(P)-\bar{u}_{j_2}^{(+)}(P)\bar{u}_{j_1}^{(-)}(P)\}] \\ \times \sum_{\sigma=\pm} [2\pi\theta(p_0)\bar{u}_{i_3}^{(\sigma)}(P)u_{j_3}^{(\sigma)}(P)], \quad (4.15)$$

where the spinors with suffices i_1, i_2 , and i_3 (j_1, j_2 , and j_3) are attached to the vertices in S (S^*).

We shall show that

$$\text{Eq. (4.15)} = \mathcal{S}_{j_1j_2j_3}^{i_1i_2i_3}(P) - \mathcal{S}_{j_1j_2j_3}^{i_2i_1i_3}(P), \quad (4.16)$$

where

$$\mathcal{S}_{j_1j_2j_3}^{i_1i_2i_3}(P) \\ \equiv (iS_{12}^{(+)}(P))_{i_1j_1}(iS_{12}^{(+)}(P))_{i_2j_2}(iS_{21}^{(+)}(P))_{j_3i_3} \\ + (iS_{11}^{(T)(+)}(P))_{i_1i_3}(iS_{12}^{(+)}(P))_{i_2j_2}(iS_{22}^{(T)(+)}(P))_{j_3j_1} \\ + (iS_{12}^{(+)}(P))_{i_1j_1}(iS_{11}^{(T)(+)}(P))_{i_2i_3}(iS_{22}^{(T)(+)}(P))_{j_3j_2}. \quad (4.17)$$

We shall prove this by running in the opposite direction; i.e., starting from Eq. (4.16), we derive Eq. (4.15). The first term on the RHS of Eq. (4.17) consists of two terms; one is proportional to n_F^2 and one is proportional to n_F^3 . The second and third terms are proportional to n_F^3 . Here $(iS_{12}^{(+)}(P))_{i_1j_1}$ may be written as [cf. Eq. (4.4)]

$$(iS_{12}^{(+)}(P))_{i_1j_1} = -2\pi n_F(p)\delta(P^2) \sum_{\sigma=\pm} u_{i_1}^{(\sigma)}(P)\bar{u}_{j_1}^{(\sigma)}(P). \quad (4.18)$$

Other S 's in Eq. (4.17) may be expressed similarly. Straightforward but tedious manipulation shows that the ‘‘ n_F^3 part’’ of $\mathcal{S}_{j_1j_2j_3}^{i_1i_2i_3} - \mathcal{S}_{j_1j_2j_3}^{i_2i_1i_3}$ vanishes. Then, in Eq. (4.16), we are left with ‘‘ n_F^2 part,’’ which turns out to be Eq. (4.15).

The same comment as above after Eq. (4.14) applies here.

(d) $\{i_{\mathbf{k}}^{(+)}=i_{\mathbf{k}}^{(-)}=j_{\mathbf{k}}^{(+)}=j_{\mathbf{k}}^{(-)}=i_{\mathbf{k}}^{(+)' }=i_{\mathbf{k}}^{(-)' }=j_{\mathbf{k}}^{(+)' }=j_{\mathbf{k}}^{(-)' }=1\}$ and its relatives. We extract

$$n_F^2 [2\pi\theta(p_0)\{u_{i_1}^{(+)}(P)u_{i_2}^{(-)}(P)-u_{i_1}^{(-)}(P)u_{i_2}^{(+)}(P)\}] \\ \times [2\pi\theta(p_0)\{\bar{u}_{j_1}^{(+)}(P)\bar{u}_{j_2}^{(-)}(P)-\bar{u}_{j_1}^{(-)}(P)\bar{u}_{j_2}^{(+)}(P)\}] \\ \times [2\pi\theta(p_0)\{\bar{u}_{i_3}^{(+)}(P)\bar{u}_{i_4}^{(-)}(P)-\bar{u}_{i_3}^{(-)}(P)\bar{u}_{i_4}^{(+)}(P)\}] \\ \times [2\pi\theta(p_0)\{u_{j_3}^{(+)}(P)u_{j_4}^{(-)}(P)-u_{j_3}^{(-)}(P)u_{j_4}^{(+)}(P)\}]. \quad (4.19)$$

As in the above case (c), through straightforward but tedious calculation, we obtain

$$\text{Eq. (4.19)} = \mathcal{S}_{j_1 j_2 j_3 j_4}^{i_1 i_2 i_3 i_4}(P) - \mathcal{S}_{j_1 j_2 j_3 j_4}^{i_2 i_1 i_3 i_4}(P) - \mathcal{S}_{j_1 j_2 j_4 j_3}^{i_1 i_2 i_3 i_4}(P) + \mathcal{S}_{j_1 j_2 j_4 j_3}^{i_2 i_1 i_3 i_4}(P), \quad (4.20)$$

where

$$\begin{aligned} \mathcal{S}_{j_1 j_2 j_3 j_4}^{i_1 i_2 i_3 i_4}(P) &\equiv (iS_{12}^{(+)}(P))_{i_1 j_1} (iS_{12}^{(+)}(P))_{i_2 j_2} (iS_{21}^{(+)}(P))_{j_3 i_3} (iS_{21}^{(+)}(P))_{j_4 i_4} \\ &+ (iS_{11}^{(T)(+)}(P))_{i_1 i_3} (iS_{12}^{(+)}(P))_{i_2 j_2} (iS_{22}^{(T)(+)}(P))_{j_3 j_1} (iS_{21}^{(+)}(P))_{j_4 i_4} \\ &+ (iS_{12}^{(+)}(P))_{i_1 j_1} (iS_{11}^{(T)(+)}(P))_{i_2 i_3} (iS_{22}^{(T)(+)}(P))_{j_3 j_2} (iS_{21}^{(+)}(P))_{j_4 i_4} \\ &+ (iS_{12}^{(+)}(P))_{i_1 j_1} (iS_{21}^{(+)}(P))_{j_3 i_3} (iS_{11}^{(T)(+)}(P))_{i_2 i_4} (iS_{22}^{(T)(+)}(P))_{j_4 j_2} \\ &+ (iS_{11}^{(T)(+)}(P))_{i_1 i_4} (iS_{12}^{(+)}(P))_{i_2 j_2} (iS_{21}^{(+)}(P))_{j_3 i_3} (iS_{22}^{(T)(+)}(P))_{j_4 j_1} \\ &+ (iS_{11}^{(T)(+)}(P))_{i_1 i_4} (iS_{11}^{(T)(+)}(P))_{i_2 i_3} (iS_{22}^{(T)(+)}(P))_{j_4 j_1} (iS_{22}^{(T)(+)}(P))_{j_3 j_2}. \end{aligned}$$

The same comment as above after Eq. (4.14) applies here.

There remains the following two configurations to be analyzed: (e) $\{i_{\mathbf{k}}^{(+)\prime} = i_{\mathbf{k}}^{(-)\prime} = j_{\mathbf{k}}^{(+)\prime} = j_{\mathbf{k}}^{(-)\prime} = 1\}$ and its relatives and (f) $\{i_{\mathbf{k}}^{(+)\prime} = i_{\mathbf{k}}^{(-)\prime} = j_{\mathbf{k}}^{(+)\prime} = j_{\mathbf{k}}^{(-)\prime} = 1, i_{\mathbf{k}}^{(\sigma)} = j_{\mathbf{k}}^{(\sigma)} = 1\}$ ($\sigma = \pm$) and its relatives. The case (e) [(f)] may be analyzed in a similar manner as (b) [(c)] above and the ‘‘right combination’’ of thermal propagators is extracted.

As in the scalar-field case, Sec. III B, there appear disconnected \mathcal{N} 's: $\mathcal{N} = \mathcal{N}_{con} \mathcal{D}$ with $\mathcal{D} \neq 1$. Such cases are treated in the same manner as in the scalar-field case.

This completes the analysis of all mode-overlapping configurations.

Conversely, we take a diagram for A in the reaction-rate formula [cf. Eq. (3.14)]. The amplitude A contains ‘‘vanishing contributions,’’ which *should* vanish. By this we mean the contributions coming from the configurations, in which at least one of $i_{\mathbf{k}}^{(\sigma)}$, $i_{\mathbf{k}}^{(\sigma)\prime}$, $j_{\mathbf{k}}^{(\sigma)}$, $j_{\mathbf{k}}^{(\sigma)\prime}$, $\bar{i}_{\mathbf{k}}^{(\sigma)}$, $\bar{i}_{\mathbf{k}}^{(\sigma)\prime}$, $\bar{j}_{\mathbf{k}}^{(\sigma)}$, $\bar{j}_{\mathbf{k}}^{(\sigma)\prime}$ ($\sigma = \pm$) is equal to or greater than 2. Let us show that such contributions really vanish. Suppose that A contains

$$\prod_{k=1}^3 (iS_{12}(R_k))_{i_k j_k}, \quad (4.21)$$

where R_k ($k=1,2,3$) is the loop momentum [cf. Eq. (3.15)] and the suffix $i_k j_k$ stands for the (i_k, j_k) element of iS_{12} in the 4×4 Dirac-matrix space. In the loop-momentum space, there are ‘‘points,’’ where $R_1 = R_2 = R_3 \equiv R = (r_0, \mathbf{r})$. Adding the contributions from the five relative diagrams, we have, in place of Eq. (4.21),

$$\sum_{perm} \sigma_{l_1 l_2 l_3}^{j_1 j_2 j_3} \prod_{k=1}^3 (iS_{12}(R))_{i_k l_k}, \quad (4.22)$$

where the summation is taken over all permutations of $(j_1 j_2 j_3)$. Here $\sigma_{l_1 l_2 l_3}^{j_1 j_2 j_3} = +$ or $-$ when $(l_1 l_2 l_3)$ is an even or

odd permutation of $(j_1 j_2 j_3)$, which is a reflection of the anticommutativity of fermion fields. We take the case $r_0 > 0$. The ‘‘type-1 side’’ of Eq. (4.22) comes from $i_{\mathbf{k}}^{(+)} + i_{\mathbf{k}}^{(-)} = 3$, and then $i_{\mathbf{k}}^{(+)} \geq 2$ or $i_{\mathbf{k}}^{(-)} \geq 2$. Then the contribution under consideration *should* vanish. In order to see that this is really the case, using the expression (4.18), we further extract, from Eq. (4.22),

$$\sum_{perm} \sigma_{l_1 l_2 l_3}^{j_1 j_2 j_3} \prod_{k=1}^3 \left[\sum_{\sigma_k = \pm} u_{i_k}^{(\sigma_k)}(R) \bar{u}_{l_k}^{(\sigma_k)}(R) \right]. \quad (4.23)$$

Again straightforward but tedious manipulation shows that Eq. (4.23) in fact vanishes. In a similar manner, we can show that Eq. (4.22) with $r_0 < 0$ also vanishes.

We can also see that the product of thermal propagators $(iS_{11}^{(T)}(R))_{i_1 j_1} \prod_{k=2}^3 (iS_{12}(R))_{i_k j_k}$ and its relatives add up to vanish. When the product of n (≥ 4) $iS_{12}(R)$ and/or $iS_{11}^{(T)}(R)$ appears in A , pick out three of them and apply the above argument to show that the contribution vanishes.

The above analysis applies to all other ‘‘vanishing contributions,’’ which include $\prod_{k=1}^3 (iS_{21}(R_k))$ with its relatives, etc. This completes the proof of absence of the ‘‘vanishing contributions.’’

V. RATE OF REACTIONS BETWEEN THE CONSTITUENT PARTICLES OF THE HEAT BATH

In the heat bath composed of scalar fields ϕ 's, taking place is the reaction

$$\begin{aligned} &\phi(\mathbf{p}_1) + \cdots + \phi(\mathbf{p}_m) + \text{heat bath} \\ &\rightarrow \phi(\mathbf{q}_1) + \cdots + \phi(\mathbf{q}_n) + \text{anything}, \end{aligned} \quad (5.1)$$

where ϕ 's are the constituent particle of the heat bath. One can easily show that the reaction rate takes the form

$$\frac{1}{V} \left(\prod_{j=1}^n 2q_j V \right) \mathcal{R} = \left(\prod_{i=1}^m \frac{1}{2p_i V} \right) \left(\prod_{i=1}^m n_B(p_i) \right) \left(\prod_{j=1}^n \{1 + n_B(q_j)\} \right) \times A(P_1^{(2)}, \dots, P_m^{(2)}, Q_1^{(1)}, \dots, Q_n^{(1)}; P_1^{(1)}, \dots, P_m^{(1)}, Q_1^{(2)}, \dots, Q_n^{(2)}), \quad (5.2)$$

where A is the RTF amplitude for the forward process,

$$\begin{aligned} & \phi_1(P_1) + \dots + \phi_1(P_m) + \phi_2(Q_1) + \dots + \phi_2(Q_n) \\ & \rightarrow \phi_2(P_1) + \dots + \phi_2(P_m) + \phi_1(Q_1) + \dots + \phi_1(Q_n). \end{aligned} \quad (5.3)$$

It is worth noting that Eq. (5.2) may be rewritten as

$$\begin{aligned} \frac{1}{V} \mathcal{R} &= \left[\prod_{i=1}^m \frac{1}{V} \int \frac{dp_{i0}}{2\pi} \theta(p_{i0}) iD_{12}(P_i) \right] \\ & \times \left[\prod_{j=1}^n \frac{1}{V} \int \frac{dq_{j0}}{2\pi} \theta(q_{j0}) iD_{21}(Q_j) \right] A \\ & \equiv \tilde{A}_{bubble}. \end{aligned} \quad (5.4)$$

The RHS, \tilde{A}_{bubble} , is a no-leg thermal amplitude, in which no summation is taken over \mathbf{p}_i ($i=1, \dots, m$) and \mathbf{q}_j ($j=1, \dots, n$).

Generalization of the above result to the theories with gauge bosons and/or fermions is straightforward.

VI. DETAILED BALANCE

In this section, on the basis of the generalized reaction-rate formula, Eq. (5.2), we derive the detailed-balance formula *through diagrammatic analysis*.

The purpose of this section is to show that the rate (5.2) for the process (5.1) is equal to the rate for the inverse process to Eq. (5.1). (For the case of theories with gauge bosons and/or fermions, the same result is obtained.) This is well known for the cases of decay and production processes, which correspond to $m=1, n=0$ and $m=0, n=1$, respectively, in Eq. (5.2).

Take a diagram for A , Eq. (5.2), and let N_1 and N_2 be the number of iD_{21} 's and iD_{12} 's, respectively, which is involved in A ,

$$\prod_{j=1}^{N_1} iD_{21}(R_j) \prod_{k=1}^{N_2} iD_{12}(R_{N_1+k}). \quad (6.1)$$

By cutting all the lines iD_{12} 's and iD_{21} 's, we divide A into one or several "type-1 islands" and one or several "type-2 islands." Here, the type-1 (type-2) island is a "maximal" *amputated* subdiagram of A , which consists of only type-1 (type-2) vertices and of the propagators iD_{11} 's (iD_{22} 's) connecting them. Then, a type-1 (type-2) island includes no type-2 (type-1) vertex. A type-1 (type-2) island is connected by iD_{21} 's and/or iD_{12} 's to type-2 (type-1) island(s).

Take a type-1 island and we write its contribution (to A)

$$\mathcal{I}_1(Q_{j_1}, \dots, Q_{j_{\ell'}}; P_{i_1}, \dots, P_{i_{\ell}}). \quad (6.2)$$

Here $\{P_{i_k}, 1 \leq k \leq \ell\}$ is a subset of $\{P_i, 1 \leq i \leq m\}$ on the LHS of Eq. (5.3) and $\{Q_{j_k}, 1 \leq k \leq \ell'\}$ is a subset of $\{Q_j, 1 \leq j \leq n\}$ on the RHS of Eq. (5.3), where $\ell, \ell' \geq 0$. This type-1 island is connected by $s_1 (\geq 0)$ propagators iD_{21} 's and $s_2 (\geq 0)$ propagators iD_{12} 's to one or several type-2 islands. With the help of the identity

$$D_{21}(R) = e^{\beta r_0} D_{12}(R), \quad (6.3)$$

and the momentum-conservation condition, we obtain, for iD 's that are attached to \mathcal{I}_1 ,

$$\begin{aligned} & \prod_{j=1}^{s_1} iD_{21}(R_j) \prod_{k=1}^{s_2} iD_{12}(R_{s_1+k}) \\ & = \exp \left(\beta \left[\sum_{k=1}^{\ell} p_{i_k} - \sum_{k=1}^{\ell'} q_{j_k} \right] \right) \prod_{j=1}^{s_1} iD_{12}(R_j) \\ & \times \prod_{k=1}^{s_2} iD_{21}(R_{s_1+k}). \end{aligned} \quad (6.4)$$

We now take a type-2 island, whose contribution is written as

$$\mathcal{I}_2(P_{i_1}, \dots, P_{i_{\ell}}; Q_{j_1}, \dots, Q_{j_{\ell'}}), \quad (6.5)$$

where $\{Q_{j_k}, 1 \leq k \leq \ell'\}$ is a subset of $\{Q_j, 1 \leq j \leq n\}$ on the LHS of Eq. (5.3) and $\{P_{i_k}, 1 \leq k \leq \ell\}$ is a subset of $\{P_i, 1 \leq i \leq m\}$ on the RHS of Eq. (5.3). Here ℓ (ℓ') is not necessarily equal to ℓ (ℓ') in Eq. (6.2). In a similar manner as above, in place of Eq. (6.4), we have, with obvious notation,

$$\begin{aligned} & \prod_{j=1}^{s'_1} iD_{21}(R_j) \prod_{k=1}^{s'_2} iD_{12}(R_{s'_1+k}) \\ & = \exp \left(\beta \left[\sum_{k=1}^{\ell} p_{i_k} - \sum_{k=1}^{\ell'} q_{j_k} \right] \right) \prod_{j=1}^{s'_1} iD_{12}(R_j) \\ & \times \prod_{k=1}^{s'_2} iD_{21}(R_{s'_1+k}). \end{aligned} \quad (6.6)$$

For all the islands, we make the above replacements; i.e., the LHS of Eqs. (6.4) and (6.6) are replaced with the respective RHS. Through this procedure, each iD_{21} and each iD_{12} in Eq. (6.1) is "used" twice. Then we obtain

$$\begin{aligned} \text{Eq. (6.1)} &= \exp \left(\beta \left[\sum_{j=1}^m p_j - \sum_{j=1}^n q_j \right] \right) \\ & \times \prod_{j=1}^{N_1} iD_{12}(R_j) \prod_{k=1}^{N_2} iD_{21}(R_{N_1+k}). \end{aligned}$$

Now we note that the propagators in \mathcal{I}_1 's (\mathcal{I}_2 's) are iD_{11} 's (iD_{22} 's), and vertices in \mathcal{I}_1 's (\mathcal{I}_2 's) are $i\lambda$ ($-i\lambda$) [cf. above after Eq. (3.13)]. Then, using the relation (3.11),

$$[iD_{11}(R)]^* = iD_{22}(R),$$

and $[i\lambda]^* = -i\lambda$, we easily see that³

$$\begin{aligned} & A(P_1^{(2)}, \dots, P_m^{(2)}, Q_1^{(1)}, \dots, Q_n^{(1)}; P_1^{(1)}, \dots, P_m^{(1)}, Q_1^{(2)}, \dots, Q_n^{(2)}) \\ &= \exp\left(\beta\left[\sum_{i=1}^m p_i - \sum_{j=1}^n q_j\right]\right) A(Q_1^{(2)}, \dots, Q_n^{(2)}, P_1^{(1)}, \dots, P_m^{(1)}; Q_1^{(1)}, \dots, Q_n^{(1)}, P_1^{(2)}, \dots, P_m^{(2)}). \end{aligned} \quad (6.8)$$

Using Eq. (6.3), we obtain

$$\begin{aligned} e^{\beta p_i n_B(p_i)} &= 1 + n_B(p_i), \\ e^{-\beta q_j \{1 + n_B(q_j)\}} &= n_B(q_j). \end{aligned} \quad (6.9)$$

Substituting Eq. (6.8) into Eq. (5.2) and using Eq. (6.9), we finally obtain

$$\frac{1}{V} \left(\prod_{j=1}^n 2q_j V \right) \mathcal{R} = \frac{1}{V} \left(\prod_{i=1}^m 2p_i V \right) \mathcal{R}'. \quad (6.10)$$

Here, the LHS is the rate of the thermal reaction (5.1) while the RHS is the rate of its inverse process

$$\begin{aligned} & \phi(\mathbf{q}_1) + \dots + \phi(\mathbf{q}_n) + \text{heat bath} \\ & \rightarrow \phi(\mathbf{p}_1) + \dots + \phi(\mathbf{p}_m) + \text{anything}. \end{aligned}$$

Equation (6.10) is the desired detailed-balance formula.

VII. $T \rightarrow 0$ LIMIT AND CUTKOSKY RULES

In this section, we show that, in the limit $T \rightarrow 0$, the reaction-rate formula (3.14) reduces to the formula that is obtained using the Cutkosky rules. Then, in the case of $m=2$ and $n=0$, Eq. (3.14) goes to the optical theorem and, for $m=2$ and $n=1$, Eq. (3.14) goes to the Mueller formula [20] for inclusive reactions.

³A comment on QCD (QED) is in order. As to the 4-gluon vertex, when compared to the scalar theory, no new feature arises. Let \mathcal{V}_i ($i=1,2$) be the factor that is associated with a trigluon vertex in a type- i island. \mathcal{V}_i is real and $\mathcal{V}_2 = -\mathcal{V}_1$. Then, in place of Eq. (6.7), we have $\mathcal{I}_1^* = (-)^N \mathcal{I}_2$ with N the number of trigluon vertices in \mathcal{I}_1 . Since A in Eq. (5.2) contains an even number of trigluon vertices, Eq. (6.8) holds unchanged. Let us turn to analyze the quark-gluon vertex. In a standard notation, the factor associated with a quark-gluon vertex in a type-1/2 island is $\pm ig \gamma^\mu T^a$. Taking a trace, in A in Eq. (5.2), of the products of γ matrices and of color matrices yields a real function of P 's and Q 's. Then, $(ig)^* = -ig$ leads to Eq. (6.8). To sum up, Eq. (6.8) holds for QCD (QED).

$$\begin{aligned} & [\mathcal{I}_1(Q_{j_1}, \dots, Q_{j_{\rho'}}; P_{i_1}, \dots, P_{i_{\rho'}})]^* \\ &= \mathcal{I}_2(Q_{j_1}, \dots, Q_{j_{\rho'}}; P_{i_1}, \dots, P_{i_{\rho'}}). \end{aligned} \quad (6.7)$$

Here we note that, from the first-principles derivation above, it is obvious that, to any order of perturbation series, the amplitude A in Eq. (5.2) is real, provided that all the contributing diagrams are added. This fact, together with Eq. (6.7), shows that

In the previous section, for a given diagram for A in Eq. (3.14), we have defined a set of ‘‘islands.’’ The islands in the set may be classified into two groups. The first group consists of islands which contain at least one external vertex. Here the external vertex is the vertex, in which or from which the external momentum flows. The second group consists of isolated islands which have no external vertex.

Let us take the scalar-field theory and investigate the zero-temperature limit ($T \rightarrow 0$) of the reaction-rate formula, Eq. (3.14). (Again, generalization to other theories is straightforward.) In this limit, $iD_{21}(P) \rightarrow 2\pi\theta(p_0)\delta(P^2)$ and $iD_{12}(P) \rightarrow 2\pi\theta(-p_0)\delta(P^2)$. It can readily be seen that, due to momentum conservation, \mathcal{I}_1 and \mathcal{I}_2 , Eqs. (6.2) and (6.5), corresponding to the isolated islands vanish. Then, the nonvanishing amplitude A contains only the islands belonging to the first group. Thus, we obtain

$$\begin{aligned} A &= \prod_{j=1}^s [2\pi\theta(r_{j0})\delta(R_j^2)] \prod_{i=1}^{N_1} \mathcal{I}_1(\{P\}_i; \{Q\}_i) \\ &\times \prod_{j=1}^{N_2} \mathcal{I}_2(\{Q\}_j; \{P\}_j), \end{aligned} \quad (7.1)$$

where $\{P\}_i$, etc., denotes the subset of P_1, \dots, P_m , which flow in the i th ‘‘type-1 island,’’ etc. $\{P\}_i \cup \{Q\}_i$ and $\{Q\}_j \cup \{P\}_j$ are not empty. In Eq. (7.1), the direction of all the s momenta, R 's, each of which connects a ‘‘type-1 island’’ and a ‘‘type-2 island,’’ is taken to flow from the ‘‘type-1 island’’ to the ‘‘type-2 island.’’ As noted before, the diagram representing A in Eq. (7.1) is connected.

The RHS of Eq. (7.1) is just the quantity which is obtained by applying the Cutkosky rules [11] (in vacuum theory) to the present case. As a special case, consider Eq. (7.1) with $m=2$ and $n=0$. Since the particle represented by ϕ is stable at $T=0$, in Eq. (7.1), $N_1 = N_2 = 1$ and $\{P\}_{i=1} = \{P\}_{j=1} = \{P_1, P_2\}$. Thus Eq. (7.1) is the optical theorem in vacuum theory. Similarly, for $m=2$ and $n \geq 1$, Eq. (7.1) is just the (generalized) Mueller formula [20] for the inclusive process,

$$\Phi(\mathbf{p}_1) + \Phi(\mathbf{p}_2) \rightarrow \Phi(\mathbf{q}_1) + \dots + \Phi(\mathbf{q}_n) + \text{anything}.$$

VIII. THERMAL CUTTING RULES

In view of the controversy mentioned in Sec. I, we survey in this section the discussions made in the past for the thermal Cutkosky formula and thermal cutting rules. Although no new result is involved here, it is worth pigeonholing the issue. The Cutkosky formula [11] in vacuum theory is the formula that relates the imaginary or absorptive part of an amplitude A to the sum of cut amplitudes $\sum_{\text{cuts}} B^{(\text{cut})}$. For simplicity, in this section, we take a self-interacting complex scalar-field theory. Generalization to other theories are straightforward. $B^{(\text{cut})}$'s are constructed from A by so cutting the propagators iD 's in A that A is divided into A_S and A_{S^*} , which are amputated. Here A_S is a part(s) of A and A_{S^*} is the complex conjugate of the amplitude that is obtained from A by removing A_S and iD 's. Cutting the propagator $iD(P)$ makes $iD(P)$,

$$2\pi\theta(\pm p_0)\delta(P^2 - m^2), \quad (8.1)$$

where the upper (lower) sign is taken when P flows from a vertex in A_S (A_{S^*}) to a vertex in A_{S^*} (A_S). When the Cutkosky formula is applied to a forward amplitude A , we see that $\text{Im}A$ is proportional to the corresponding reaction rate, where cutted propagators represent the (on-shell) particles in the final state.

Kobes and Semenov (KS) [12] were the first who generalized the Cutkosky formula to the case of the RTF. Namely, they obtained the formula that relates the imaginary part of a thermal amplitude to the sum of ‘‘circled amplitudes,’’ each of which corresponds to the ‘‘circled’’ diagram that includes the so-called circled and uncircled vertices. The first paper of [12] discusses general thermal amplitudes and the second one discusses physical amplitudes, i.e., amplitudes with all external vertices being of type 1. In the sequel, unless otherwise stated, we shall restrict our concern to the physical amplitudes. The thermal Cutkosky formula deduced in [12] may be written in terms of thermal amplitudes in the RTF:

$$\begin{aligned} & \text{Im}[iG(P_1^{(1)}, \dots, P_n^{(1)})] \\ &= -\frac{1}{2} \sum'_{i_1, \dots, i_n=1}^2 G(P_1^{(i_1)}, \dots, P_n^{(i_n)}). \end{aligned} \quad (8.2)$$

Here $G(P_1^{(i_1)}, \dots, P_n^{(i_n)})$ stands for the (amputated) thermal amplitude with type- i_j ($j=1, \dots, n$) external vertices in which or from which P_j flows. In Eq. (8.2), the sum \sum' stands for taking summation excluding $i_1 = \dots = i_n = 1$ and $i_1 = \dots = i_n = 2$. Note that, as a matter of course, in G , the sum is taken over the types (1 and 2) for all internal vertices.

KS then generalized the notion of cuttings. Comparison of $iD_{21}(P)$, Eq. (3.10), and $iD_{12}(P) = iD_{21}(-P)$, Eq. (3.12), with Eq. (8.1) leads them to regard iD_{12} and iD_{21} in G 's on the RHS of Eq. (8.2) as *cut propagators*. Through cuttings, each G is divided into several pieces. KS then introduced a notion of *cuttable* and *uncuttable diagrams*. The former diagram is the diagram that does not include isolated island(s) (cf. Sec. VII) while the latter diagram includes at least one isolated island. Note that, in the case of vacuum theory, all the diagrams are cuttable ones, which motivates KS to introduce the above definition. Thus, the terminology ‘‘uncut-

table’’ sounded quite natural at the time of its introduction. In spite of the fact that this is a matter of definition, the existence of *uncuttable diagrams* has aroused controversy.

Kobes analyzed [13] retarded Green functions in terms of circled diagrams. As to the usage of ‘‘cuttings,’’ ‘‘cuttable,’’ and ‘‘uncuttable,’’ he followed [12].

Jeon analyzed [14] two-point functions in imaginary-time formalism. Continuing to the real energies, he discussed thermal cutting rules. His definition of cutting is the same as in [12]; i.e., the propagators iD_{12} and iD_{21} are regarded as cut propagators. No mention was made on the cuttable and uncuttable diagrams, but no doubt that he supposed all diagrams to be cuttable.

Bedeque, Das, and Naik analyzed [15] the imaginary part of thermal amplitudes (physical and ‘‘unphysical’’) from the same starting formula as in [12], but with a different route. Recall that the propagator iD_{jk} ($j, k=1, 2$) connects a type- j vertex with a type- k vertex. iD_{jk} is defined to be a *cut propagator* if and only if one of the type- j and type- k vertices is of circled and another is of uncircled (cf. the first paper of [12]). They then showed that the imaginary part of a thermal amplitude is written as the sum of *cuttable diagrams*, in the sense of KS stated above. In each cuttable diagram, a connected subdiagram(s) at one side of the cut line contains only uncircled vertices (external and internal) while a connected subdiagram(s) at the other side of the cut line contains only circled vertices. As was pointed out in [16], however, each connected part contains in general propagators that are proportional to the on-shell factor $\delta(P^2 - m^2)$. Of course, in the zero-temperature limit, their formula as well as KS's one reduce to the Cutkosky formula.

Gelis extensively analyzed [16] thermal cutting rules for various formulations of real-time thermal field theory. As to the usage of ‘‘cuttings,’’ ‘‘cuttable,’’ and ‘‘uncuttable,’’ he followed [12].

Cutting rules for thermal reaction-rate formula are discussed in [2–7]. Note that, as mentioned above, in vacuum theory, the cut propagator, Eq. (8.1), corresponds to the (on-shell) final-state particle. The thermal cutting rules introduced in [2–7] are a generalization of this fact. As we have seen above, iG_{12} (which collectively denotes iD_{12} and iS_{12}) (iG_{21}) consists of two parts; one comes from the particle (antiparticle) in the initial state and the other comes from the antiparticle (particle) in the final state, while $iG_{11}^{(T)}$ and $iG_{22}^{(T)}$, the T -dependent parts of iG_{11} and iG_{22} , come from the interplay of the initial-state (anti)particle and the final-state (anti)particle. We recall that each of the thermal propagators iG_{11} and iG_{22} consists of two parts, the $T=0$ part $iG^{(0)}$ and the T -dependent part $iG^{(T)}$. Then, A in Eq. (3.14) or (5.2) is divided into 2^N contributions, where N is the number of iG_{11} 's and iG_{22} 's. The above observation leads us to regard iG_{12} , iG_{21} , $iG_{11}^{(T)}$, and $iG_{22}^{(T)}$ as the *cut propagators*.

Through the applications of the above cutting rules, A is divided into several subparts. Each subpart contains only type-1 vertices or only type-2 vertices. The former (latter) belongs to S (S^*) in $\langle S^*S \rangle$. The cuttings work as follows. The line that cut $iG_{12}(P)$ with $p_0 > 0$ ($p_0 < 0$) is the initial-state particle (final-state antiparticle) cut line. The line that cut $iG_{21}(P)$ with $p_0 > 0$ ($p_0 < 0$) is the final-state particle

(initial-state antiparticle) cut line. The line that cut $iG_{11}^{(T)}(P)$ [$iG_{22}^{(T)}(P)$] is the initial-state cut line *and* the final-state cut line in S (S^*) and, in S^* (S), one extra spectator particle with P is, for the line that cut $iG_{11}^{(T)}(P)$ with $p_0 > 0$ ($p_0 < 0$) is the initial-state particle (antiparticle) cut line *and* the final-state particle (antiparticle) cut line. For the cut line on $iG_{22}^{(T)}(P)$, a similar statement holds.

It is quite obvious that the ‘‘cutting rules’’ introduced above for thermal reaction rates may be used for general thermal amplitudes evaluated in the Keldish variant of the RTF.

Finally, it is worth mentioning that it can easily be seen from Eqs. (3.14) and (8.2) that the RHS of Eq. (8.2), which represents the imaginary part of a physical amplitude, is a sum of various reaction rates times corresponding kinematical factors.

ACKNOWLEDGMENTS

This work was supported in part by the Grant-in-Aide for Scientific Research [(A)(1) (No. 08304024)] of the Ministry of Education, Science and Culture of Japan.

APPENDIX: PROOF OF EQ. (3.24)

Here we prove the identity Eq. (3.24). We expand the RHS of Eq. (3.24) in powers of $n_B(x) (\equiv \xi)$ to obtain

$$\begin{aligned} & \sum_{k=0}^{\min(j,j')} \frac{i!}{(i-j+k)!} \frac{i'!j'!}{(j'-k)!} \binom{j}{k} \xi^{i+k} (1+\xi)^{j'-k} \\ &= \sum_{k=0}^{\min(j,j')} \sum_{\ell=0}^{j'-k} \frac{i!}{(i-j+k)!} \\ & \quad \times \frac{i'!}{\ell!(j'-k-\ell)!} \frac{j!j'!}{k!(j-k)!} \xi^{i+j'-\ell} \\ &= \sum_{k=0}^{j'} \sum_{\ell=0}^{\min(j'-k,j)} \frac{i!}{(i-j+\ell)!} \frac{j!}{\ell!(j-\ell)!} \\ & \quad \times \frac{i'!j'!}{k!(j'-k-\ell)!} \xi^{i+i'-k}, \end{aligned} \quad (A1)$$

where $i \geq j$. Comparing Eq. (A1) with Eq. (3.23), we see that it is sufficient to show that

$${}^k \mathcal{F}_{j,j'}^{i,i'} = {}^k \mathcal{G}_{j,j'}^{i,i'}, \quad (A2)$$

where

$${}^k \mathcal{F}_{j,j'}^{i,i'} \equiv \sum_{\ell=0}^{\min(j,j'-k)} \frac{i!j!}{\ell!(i-j+\ell)!(j'-k-\ell)!(j-\ell)!}, \quad (A3)$$

$${}^k \mathcal{G}_{j,j'}^{i,i'} \equiv \frac{(j+i'-k)!}{(i'-k)!(j'-k)!}. \quad (A4)$$

Here we define two functions:

$$F_{j,j'}^{i,i'}(x) \equiv \sum_{k=0}^{j'} x^{j'-k} {}^k \mathcal{F}_{j,j'}^{i,i'}, \quad (A5)$$

$$G_{j,j'}^{i,i'}(x) \equiv \sum_{k=0}^{j'} x^{j'-k} {}^k \mathcal{G}_{j,j'}^{i,i'}. \quad (A6)$$

It can easily be shown that F 's and G 's satisfy the same differential equation:

$$\frac{d}{dx} F_{j,j'}^{i,i'}(x) = F_{j,j'-1}^{i,i'-1}(x) + j F_{j-1,j'-1}^{i,i'}(x), \quad (A7)$$

$$\frac{d}{dx} G_{j,j'}^{i,i'}(x) = G_{j,j'-1}^{i,i'-1}(x) + j G_{j-1,j'-1}^{i,i'}(x). \quad (A8)$$

From Eqs. (A5), (A6) with Eqs. (A3) and (A4), we obtain

$$F_{j,j'}^{i,i'}(0) = G_{j,j'}^{i,i'}(0) = \frac{i!}{(i-j)!}, \quad (A9)$$

$$F_{j,0}^{i,i'}(x) = G_{j,0}^{i,i'}(x) = \frac{i!}{(i-j)!}. \quad (A10)$$

We see from Eq. (A7) [Eq. (A8)] that $F_{j,j'}^{i,i'}(x)$ [$G_{j,j'}^{i,i'}(x)$] may be obtained from $F_{\hat{j},0}^{i,\hat{i}'}(x)$ [$G_{\hat{j},0}^{i,\hat{i}'}(x)$] in Eq. (A10) with $\hat{i}' \leq i'$, $\hat{j} \leq j$, and $F_{\hat{j},\hat{j}'}^{i,\hat{i}'}(0)$ [$G_{\hat{j},\hat{j}'}^{i,\hat{i}'}(0)$] in Eq. (A9) with $\hat{i}' \leq i'$, $\hat{j} \leq j$, $\hat{j}' \leq j'$. Since F 's and G 's subject to the same set of equations (A7)–(A10), we conclude that

$$F_{j,j'}^{i,i'}(x) = G_{j,j'}^{i,i'}(x),$$

which proves Eq. (A2). Q.E.D.

[1] See, e.g., H. A. Weldon, Phys. Rev. D **28**, 2007 (1983).
 [2] A. Niégawa, Phys. Lett. B **247**, 351 (1990).
 [3] N. Ashida, H. Nakkagawa, A. Niégawa, and H. Yokota, Ann. Phys. (N.Y.) **215**, 315 (1992); **230**, 161(E) (1994).
 [4] N. Asida, Int. J. Mod. Phys. A **8**, 1729 (1993).
 [5] N. Ashida, H. Nakkagawa, A. Niégawa, and H. Yokota, Phys. Rev. D **45**, 2066 (1992).

[6] A. Niégawa and K. Takashiba, Ann. Phys. (N.Y.) **226**, 293 (1993); **230**, 162(E) (1994).
 [7] P. V. Landshoff, Phys. Lett. B **386**, 291 (1996).
 [8] See, e.g., N. P. Landsman and Ch. G. van Weert, Phys. Rep. **145**, 141 (1987).
 [9] M. Jacob and P. V. Landshoff, Phys. Lett. B **281**, 114 (1992).
 [10] T. S. Evans and D. A. Steer, Nucl. Phys. **B474**, 481 (1996).

- [11] R. E. Cutkosky, *J. Math. Phys.* **1**, 429 (1960); R. J. Eden, P. V. Landshoff, D. I. Olive, and J. C. Polkinghorne, *The Analytic S-Matrix* (Cambridge University Press, Cambridge, England, 1966).
- [12] R. L. Kobes and G. W. Semenoff, *Nucl. Phys.* **B260**, 714 (1986); **B272**, 329 (1986).
- [13] R. Kobes, *Phys. Rev. D* **43**, 1269 (1991).
- [14] S. Jeon, *Phys. Rev. D* **47**, 4586 (1993).
- [15] P. F. Bedaque, A. Das, and S. Naik, *Mod. Phys. Lett. A* **12**, 2481 (1997); A. Das, *Finite Temperature Field Theory* (World Scientific, Singapore, 1997).
- [16] F. Gelis, hep-ph/9701410, ENSLAPP-A-639/97.
- [17] T. Kinoshita, *J. Math. Phys.* **3**, 650 (1962); N. Ohta, *Prog. Theor. Phys.* **62**, 1370 (1979).
- [18] A. J. Niemi and G. W. Semenoff, *Ann. Phys. (N.Y.)* **152**, 105 (1984); *Nucl. Phys.* **B230**, 181 (1984).
- [19] H. Hata and T. Kugo, *Phys. Rev. D* **21**, 3333 (1980).
- [20] A. H. Mueller, *Phys. Rev. D* **2**, 2963 (1970).